doi:10.1038/nature14507

Population Genomics of Bronze Age Eurasia

Morten E. Allentoft, Martin Sikora, Karl-Göran Sjögren, Simon Rasmussen, Morten Rasmussen, Jesper Stenderup, Peter B. Damgaard, Hannes Schroeder, Torbjörn Ahlström, Lasse Vinner, Anna-Sapfo Malaspinas, Ashot Margaryan, Tom Higham, David Chivall, Niels Lynnerup, Lise Harvig, Justyna Baron, Philippe Della Casa, Paweł Dąbrowski, Paul R Duffy, Alexander V. Ebel, Andrey Epimakhov, Karin Frei, Mirosław Furmanek, Tomasz Gralak, Andrey Gromov, Stanisław Gronkiewicz, Gisela Grupe, Tamás Hajdu, Radosław Jarysz, Valeri Khartanovich, Alexandr Khokhlov, Viktória Kiss, Jan Kolář, Aivar Kriiska, Irena Lasak, Cristina Longhi, George McGlynn, Algimantas Merkevicius, Inga Merkyte, Mait Metspalu, Ruzan Mkrtchyan, Vyacheslav Moiseyev, László Paja, György Pálfi, Dalia Pokutta, Łukasz Pospieszny, T. Douglas Price, Lehti Saag, Mikhail Sablin, Natalia Shishlina, Vaclav Smrcka, Vasilii I. Soenov, Vajk Szeverényi, Gusztáv Tóth, Synaru V. Trifanova, Liivi Varul, Magdolna Vicze, Levon Yepiskoposyan, Vladislav Zhitenev, Ludovic Orlando, Thomas Sicheritz Pontén, Søren Brunak, Rasmus Nielsen, Kristian Kristiansen and Eske Willerslev

Contents

The following Supplementary tables are found as separate files:

Supplementary Table 6: Sequencing statistics

Supplementary Table 7: DNA damage

Supplementary Table 8: DNA contamination tests

Supplementary Table 10: D-test for all combinations

D(Outgroup,Ancient$_1$)(Ancient$_2$)(Ancient$_3$); 1000 Genomes dataset

Supplementary Table 11: "Outgroup" f_3-statistics for all combinations of ancient and modern groups; Human Origins dataset

Supplementary Table 12: All-pair "admixture" f_3-statistics; 1000 Genomes dataset

Supplementary Table 13: Derived allele frequencies of 104 SNP catalogue for putative selection; 1000 Genomes dataset

Supplementary Table 14: mtDNA haplogroups

Section 1

An introduction to the sampled cultures and their dating

1.1 Bronze Age - the beginning

The Bronze Age starts with urbanisation and state formation in Mesopotamia around 3000 BC but with some urbanisation already evolving during the 4th millennium BC. From that time onwards copper alloys (including bronze) were systematically used in the economy for agricultural tools, weapons, personal ornaments, metal cauldrons and cups for cooking, dining and drinking. Therefore, large quantities of copper were needed but since there are no sources of metal in Mesopotamia, all metal had to be traded in, mostly from mining areas in Caucasus and later Oman. This exploitation of copper mines in Anatolia and Caucasus had started already during the early and middle 4th millennium BC, when colonizing groups from Mesopotamia, known as the Uruk movement, settled in the north to establish new trade routes and thus securing the flow of copper, gold and silver back to the Mesopotamian heartland[1]. The ages provided below should be considered approximate as the exact time frames for the various cultures are subject to some discussion.

1.2 Maikop and Late Tripolje (3700-3000 BC), Yamnaya (3000-2400 BC), and Remedello 1 (3400-2800 BC) cultures

As a results of these colonizing ventures, prestige goods from Mesopotamia were traded into the Caucasus, where we find them earliest in the richly furnished, chiefly barrows (or kurgans in Russian) of the Maikop Culture in northern Caucasus from the middle and later part of the 4th millennium BC[2]. They represent the first ranked societies of the steppe based on a new perception of individualized property and the monogamous family. These concepts were most likely adopted from Mesopotamia along with prestige goods and metallurgy as a result of regular trade[3,4]. From the northern hills of the Caucasus this social "package", symbolized in the new burial ritual of individual (family) burials in kurgans/barrows soon spread to the steppe where it was linked to a new economy of pastoralism and herding of mainly cattle[5, 6]. The Maikop Culture produced some of the most astonishing figurines of cattle made of gold, which symbolized their use as draught animals for the earliest wheeled vehicles[7, 8]. This custom rapidly spread all the way to northern Europe.

During the 4th millennium BC, large mega settlements of up to 400 hectares with populations in the ten thousands, known as the Tripolje Culture [2, 9], emerged in the western forest-steppe, bordering the steppe. By the middle of the 4th millennium BC, it seems that such large populations could no longer be sustained and the mega-sites gradually collapsed and were left. The Tripolje populations expanded into the steppe [10] where they encountered Maikop groups and adopted individual burials under barrows and metallurgy. Horse domestication and the development of wheeled vehicles, in the style of later prairie wagons[11], took place to support a mobile pastoral lifestyle in the steppe. A new expansionist pastoral society, called the Yamnaya Culture (see below), evolved from this merging of cultures, and spread rapidly east and westwards, from Hungary to the Ural Mountains. This Yamnaya expansion has often been associated with the spread of Proto-Indo-European languages, after the early split of Anatolian/Hittite[12].

The Remedello Culture was a North Italian Copper Age Culture, situated in the Po Delta and the Italian Alps. It was contemporary with the famous Ötzi (the "Iceman"). The culture is best known from their often rich, individual burials in flat graves, sometimes with copper daggers, axes, halberds and pins. They show cultural connections with the Northern Alps, the Aegean and Anatolia.

We have in recent years witnessed a new ^{14}C-dating programme of Russian samples from burials. Due to the reservoir effects from freshwater diet, many previous ^{14}C-dates of human bone can now be demonstrated as being too old - sometimes by 300-400 years. This has been demonstrated by systematically dating objects of animal bones, or objects made from animal bone, and of short lived timber from graves[13,14,15]. We have therefore here lowered the absolute chronology of Yamnaya and related cultures in accordance with these new results.

1.3 Yamnaya (3000-2400 BC), Catacomb 2700-2300 BC), Afanasievo (2900 – 2500 BC), and Okunevo Culture (2500-1900 BC)

The new social and economic and technological package introduced by the Maikop Culture was soon adopted by steppe populations, and resulted in the formation and subsequent rapid expansion of the Yamnaya Culture between 3000-2400 BC[12]. Catacomb Culture was a regional variety with deep catacomb-shaped graves, some also found in Eastern Europe and Greece[16]. The Yamnaya, or Pit Grave Culture, is characterized by individual pit or shaft grave burials under a barrow. Sometimes decorated stone stelae were placed on top of the barrow. The economy was based on animal herding with seasonal movements between grazing grounds. As stated by Anthony (2007): "The Yamnaya horizon is the visible archaeological expression of a social adjustment to high mobility – the invention of the political infrastructure to manage larger herds from mobile homes based in the steppes"[12]. And further to the lack of settlements: "The best explanation for the complete absence of settlements is that the eastern Yamnaya spent much of their lives in wagons"[12]. Horse riding were adopted to manage the herds. Around 2900 BC, the western Yamnaya culture continued its expansion into the Carpathian basin to the Hungarian plain, as well as north of the Carpathians. To the east they reached the Urals/Trans-Urals, where the general expansion stopped for nearly a thousand years.

Despite the general Yamnaya expansion stalling at Ural, some groups must have been looking for more distant grazing grounds because in the eastern steppe of Western Siberia we find an outlier culture that seems culturally related to early Yamnaya. The archaeological explanations for this phenomenon diverge: traditionally it has been considered the result of a remarkable long-distance migration that took place at an early stage of the pre-Yamnaya (known as the Repin Culture) on the western steppe. A two-thousand-kilometre trek across the central steppe to the Altai Mountains, rich in good grazing and suited for transhumance[12]. The settlers introduced a fully developed kurgan/barrow culture and the pastoral economy known from the western steppe. This migratory route, with a few stations along the way, was maintained, and later Yamnaya groups continued to use it. This phenomenon led to the formation of the Afanasievo Culture near Altai. An alternative explanation links Afanasievo to the southwest – being part of an inner mountain corridor from Pamir to Altai - and a southwest Asian/Near Eastern source of pastoralism[17]. It has been proposed that groups from the Afanasievo Culture migrated south to Xinjang and the Tarim basin, bringing with them the Tocharian language, the

second oldest to break off from Proto-Indo-European with a western, Europan origin[19], while others would see this being part of the above mentioned interaction zone with the southwest Pamir and Hindu Kush[17]. The later Okunevo Culture was a local, south Sibirian early Bronze Age adaptation of Afanasievo influences, and is characterized by stone stelae with expressive art of a shamanistic nature[18].

1.4 Corded Ware, Battle Axe, and Single Grave cultures (2800-2300 BC)

These are different names for a series of similar cultural formations in temperate Europe during the period 2800-2300 BC [20, 21]. They shared the individual burials in pits under barrows (except in the Swedish Battle Axe Culture) with Yamnaya, and finely executed stone axes, as grave goods for male warriors, replaced the copper axes of the Yamnaya Culture. The European Corded Ware Culture groups developed a new type of fine pottery with cord decoration to hold beer. It was part of a shared drinking ritual amongst all these groups. The economy was dominantly pastoral with some elements of farming being stronger in Central Europe. The expansion of this mobile agro-pastoral economy was rapid and sometimes dramatic, as evidenced in a recently analysed multiple burial from Saxony-Anhalt, which was the result of a massacre on a small family group of thirteen individuals [22, 23, 24]. During the Early- and Middle Neolithic periods there were still large forest reserves preserved in Europe, although mainly on lighter soils. However, during the early third millennium BC these areas were colonised by expanding pastoral herders and warriors with an apparent never-ending appetite for new pastures. As evidenced in pollen diagrams, they rapidly burned down the forests to create grazing lands for their animals [25-28]. As land-use was extensive it demanded much larger tracts of open land to feed people and animals compared to a more sedentary agrarian economy, so to facilitate communication and travels they employed four-wheeled ox-drawn wagons[11].

The Corded Ware Culture (mainly in Central Europe), Single Grave Culture (mainly in Northwestern Europe) and Battle Axe Culture (in Sweden mainly) of the temperate forest zone of Europe shared the burial ritual or individual family barrows with the Yamnaya Culture, as well as a pastoral economy mixed with some farming. There can be little doubt that the western Yamnaya expansion, first into Hungary and then north of the Carpathians, was somehow involved in this social and economic transformation[29-31]. However, archaeologists have been divided about the role of large-scale migrations [32] versus local adaptations [33] in facilitating these changes. There are astonishing similarities in burial rituals across vast areas [34], which might point towards widespread migrations as the dominating force. This is in some regions supported by strontium analyses of mobility[35 36], which has also been linked to movement of women in exogamous marriage arrangements[37]. Settlements are rare in the early phase which is another indication of a nomadic lifestyle[38]. The mobile lifestyle is also exemplified by the use of mats, tents, and wagons, which are sometimes found in burials [15]. During this time the population becomes taller than previous Neolithic people and leads to a general rise in the stature of the population from the late third millennium BC and onwards. In Denmark the average height of males increases with 7 cm from the Megalith period of the late fourth millennium BC to the early Bronze Age of the late third millennium BC.

To summarize, during the third millennium BC a new social and economic order in western Eurasia arises. By the mid-third millennium BC, common rituals and social institutions were employed from the Urals to Northern Europe within the temperate lowland zone. How this

situation was brought about – its underlying social and demographic processes - is still a matter of archaeological debate.

1.5 Abashevo/Sintashta (2100-1800 BC), Andronovo (1700- 1500 BC), Karasuk (1400-900 BC), and Mezhovskaya Culture (1300-800/700 BC).

The Sintashta Culture, located in the Trans-Urals, represents the earliest, fully-developed, chariot-using Bronze Age culture. Here an enclave of highly organized fortified settlements, with a systematic layout of houses, appeared around 2100/2000 BC. The new settlements were located close to copper mines, and mining and metallurgy played an important role. The economy was mainly pastoral. Warriors and charioteers were often buried with two-wheeled chariots and two horses in shaft graves under mounds[39]. West of the Urals, stretching through the forest-steppe zone into Eastern Europe we find a related sister culture, called the Abashevo Culture, which also relied on chariots[39]. In Figure 1 (main text) we have documented the early use of chariots by black dots during the period 2000-1800 BC[40], each dot represents a chariot burial with horse cheek pieces of similar type. We can thus document the new expanding warrior elites from east Central Europe to the South-Eastern Urals, but also including Mycenae and Hittite Anatolia. A new class of master artisans emerged to build chariots, breed and train horses, produce new weapons and train others in using them. This package of skills was so complex that it demanded the transfer of people, horses and warriors to be properly adopted. Once adopted this package changed the nature of society, as it introduced a whole series of new economic and social demands, as well as a new ideology of aristocracy linked to warfare and political leadership. Thus, it represented a new institution of warrior aristocracies and their attached specialists that changed Bronze Age societies throughout Eurasia and the Near East.

Where did they come from? Archaeologically it is not possible to trace the origin of the Sintashta Culture. Recent archaeological work has clarified that the settlements represent a well-organized colonizing venture[41,42]. Many suggestions of their origin has been put forward, spanning from the Circumpontic region and Caucasus to Northern Iran[43]. After 1800/1700 BC late Sintashta populations appear to have expanded eastwards through a mix of colonization and local adaptations, forming the Andronovo Culture, which carried on the use of chariots (Figure 1, main text). They eventually migrated further south and east into northern Iran and Northern India/Pakistan where they became the new ruling elite[44,45]. From here the Rig Veda, hymns and ritual texts, probably written down between 1500-1000 BC, testify to this new warrior culture. There are many similarities between Sintasthta/Androvono rituals and those described in the Rig Veda and such similarities even extend as far as to the Nordic Bronze Age[46,47].

The Karasuk Culture represents the continuation and transformation of the Andronovo and Okunevo cultures. The influence of this culture can be traced from the Sayano-Altai to the Aral Sea, China and Western Siberia[48].

The Mezhovskaya Culture is one of the largest cultural and social formations of the final Bronze Age in the forest and forest-steppe zone of western Siberia and the Urals[39]. It shows influences from several sources – the steppe and the eastern forest zone, as well as from the KarasukCulture. Some would equate this culture with later Ugrian populations, but this is contested.

1.6 European Bronze Age Cultures: Bell Beaker (2600-2000 BC)/Unetice/Nordic LN (2300-1800 BC), Vatya (2000-1500 BC), Maros (2300-1500 BC) and Tumulus/Nordic Cultures (1700-1200 BC).

In Northern and Western Europe the Bronze Age proper starts with the expansion of so-called Bell Beaker Culture groups between 2600 and 2000 BC and the Unetice Culture (2300-1800 BC). A common view is that Bell Beaker groups expanded out of Iberia along the western Mediterranean and along the Atlantic façade before they moved inland (but never further east than Hungary), and always settled in small pockets. This scenario is based on a morphological study of teeth from 2000 European Bell Beaker individuals[49]. They were travelling artisans and probably well-received because of their skills[30,50,51], but they were also a demographic force looking for new places to settle[51]. Through hybridization between the Corded Ware/Single Grave Culture and the expanding Bell Beaker Culture, hybrid Beaker Cultures emerged in the British Isles[52] and in Central Europe [30,53]. These new cultures experienced a rapid expansion that transformed society in much the same way as the Corded Ware and Single Grave Culture had transformed temperate Europe c. 300 years earlier. However, in Central and Northern Europe, the Unetice Culture represented the first miners and metallurgists, who introduced a commodity based metal economy, implying a rather high degree of mobility within some groups[54].

After 1800/1700 BC all European societies became integrated in a full-scale commodity based copper and tin metal trade. Demographic figures for Europe now approach those of the Near East[55]. We can distinguish between two social formations: the Tumulus Culture groups stretching from South Germany to South Scandinavia based on smaller settlements of individual farms for stalling cattle, and the Tell societies of East-Central Europe, where larger populations lived together in fortified settlements over several hundred years forming a tell. In Central Hungary such settlements along the Danube are characterized first by Nagyrév Culture (2300-2000 BC), then by Vatya Culture material (2000-1500 BC), while along the Hungarian-Romanian-Serbian border such tells belong to the Maros/Mureş Culture (2300-1500 BC). From this time onwards we see less migration and more movements of traders and warriors, often over long distances. The archaeological reconstruction of such a trade network linked by strategic marriages[56] demonstrates that specific groups with specific swords, such as octagonally hilted swords and flange hilted swords, were able to move and travel long distances. This movement can now also be supported by strontium isotope analysis, such as at Neckarsulm, a cemetery of males, mainly warriors, where one third were non-local, and thus probably had travelled to take service with a foreign chief [57]. The archaeology thus suggests that organized travels between communities that were linked by political alliances were normal.

The 2nd millennium BC saw the intensification and expansion of networks created during the 3rd millennium BC by new technologies of mobility, such as chariots, and by the full-scale adaptation of bronze, leading to a more complex political economy[58]. According to Frachetti (2012): "By the second millennium BC, these incipient regional interactions fostered the spread of new and emerging technologies, cross-fertilized domestic and economic innovations, and ramped-up trade in commodities and raw materials. This growing interactive network promoted new opportunities to extend institutional codes and to capitalize on flexible regional political relationships" [17,20]. It is still a matter of uncertainty what regional demographic and cultural impact, e.g. in the form of language change, these travels and interactions would have had[59,60].

References

1 Aubet, M. E. 2013 *Commerce and Colonization in the Ancient Near East.* Cambridge University Press. Cambridge.

2 Kohl, P. 2007 The Making of Bronze Age Eurasia. Cambridge University Press.

3 Hansen, S. Hauptman, A, Motzenbäcker, I. and Pernicka, E. (eds.) 2010 *Von Majkop bis Trialeti.* Gewinnung und Verbreitung von Metallen und Obsidian in Kaukaisen im 4.-2. Jt. V. Chr. Bonn.

4 Ivanova, M. 2012 Kaukasus und Orient: Die Entstehung des "Maikop-Phänomens" im 4. Jahrtausend v. Chr. Praehistorische Zeitschrift 87(1):1-28.

5 Rezepkin, A. D. 2000 *Das frühbronzezeitliche Gräberfeld von Klady und die Majkop-Kultur in Nordwestkaukasien.* Archäologie in Eurasien, Band 10, Verlag Marie Leidorf (VML). Rahden, Westfalen.

6 Rezepkin, A. D. 2010 Metallfunde der Majkop under der Novosvobodnaja Kultur. In Hansen, S. Hauptman, A, Motzenbäcker, I. and Pernicka, E. (eds.) *Von Majkop bis Trialeti.* Gewinnung und Verbreitung von Metallen und Obsidian in Kaukasien im 4.-2. Jt. V. Chr.:95-102 Bonn.

7 Hansen, S. 2014 Gold and Silver in the Maikop Culture. In H. Meller, R. Risch and E. Pernicka (eds.): *Metals of Power – Early gold and silver*: 389-410. Tagungen des Landesmuseums für Vor-und Frühgeschichte Halle, Band 11. Halle.

8 Hansen, S. 2011 Technische und soziale Innovationen in der zweiten hälfte des 4. Jahrtausend v. Chr. In S. Hansen and J. Müller (eds.): *Sozialarchäologische Perspektiven: Gesellschaftlicher Wandel 5000-1500 v. Chr. Zwischen Atlantik und Kaukasus*: 153-191. Verlag Phillipp von Zabern. Bonn.

9 Chapman, J. et al. 2014 The Second Phase of the Trypillia Mega-Site Methodological Revolution: A New Research Agenda. *European Journal of Archaeology* 17(3):369-406.

10 Manzura, I. 2005 Steps to the steppe: or, how the north Pontic region was colonised. *Oxford Journal of Archaeology* 24(4): 313-338.

11 Burmeister, S. (ed.) 2004 *Rad und Wagen*. Der Ursprung einer Innovation. Wagen im vorderen Orient und Europa. Verlag Phillip von Zabern. Mainz am Rhein.

12 Anthony, D. 2007 *The Horse, the Wheel and Language*. How Bronze-Age riders from the Eurasian Steppes Shaped the Modern World. Princeton University Presss. Princeton and Oxford.

13 Shishlina, A. I. Et al. 2009 Paleoecology, Subsistence, and 14C Chronology of the Eurasian Steppe Bronze Age. *Radiocarbon*, Vol 51, Nr. 2:481-499.

14 Shishlina, N. I., J. Van der Plicht and E. P. Zazovskaya 2010 Radio Carbon Dating of Bronze Age Bone Pins from Eurasian Steppe. *Geochrometria* DOI 10.2478/s13386-011-0015-8

15 Shislina, N. 2008 *Reconstruction of the Bronze Age of the Caspian Steppes*. Life styles and life ways of pastoral nomads. BAR International Series 1876. Oxford.

16 Kaiser, E: 2003 Studien zur Katakombergrabkultur zwischen Dnepr und Prut. *Archäologie in Eurasien*, Band 14. Philipp von Zabern, Mainz am Rhein.

17 Frachetti, M. D. 2012 Multiregional Emergence of Mobile Pastoralism and Nonuniform Institutional Complexity across Eurasia. *Current Anthropology*, Vol. 53, No. 1:2-38.

18 Gass, A. 2011 *Frühbronzezeit am mittleren Enisej*. Gräberfelder der frühbronzezeitlichen Okunev-Kultur im Minusinsker Becken. Verlag Dr. Rudolf Habelt Gmbh: Bonn.

19 Mallory, J. P. and Mair, V. H. 2000 *The Tarim Mummies*. Ancient China and the Mystery of the Earliest People from the West. Thames & Hudson, London.

20 Kristiansen, K. 2007 Eurasian transformations: mobility, ecological change, and the

transmission of social institutions in the third millennium and the early second millennium B.C.E. In *The World System and the Earth System. Global Socioenvironmental Change and Sustainability since the Neolithic*, edited by A. Hornborg and C. Crumley, pp. 149–162. Left Coast Press, Walnut Creek, CA.

21 Milisauskas, S. And J. Kruk 2013 Late Neolithic/Late Copper Age 3500-2200 BC. In Milisauskas, S. 2013 *European Prehistory. A Survey*:chapter 9. 2nd edition. Springer.

22 Meyer, C., Brandt, G., Haaka, W., Ganslmeier, R. A., Meller, H. and Alt, K. W. 2009 The Eulau eulogy: bio-archaeological interpretation of lethal violence in Corded Ware multiple burials from Saxony-Anhalt, Germany. *Journal of Anthropological Archaeology* 28: 412–423.

23 Czebreszuk, J. and Szmyt, M. 2011 Identities, Differentiation and Interactions on the Central European Plain in the 3rd Millennium BC. In S. Hansen and J. Müller (eds.): *Sozialarchäologische Perspektiven: Gesellschaftlicher Wandel 5000-1500 v. Chr. Zwischen Atlantik und Kaukasus*: 269-291. Verlag Phillipp von Zabern. Bonn.

24 Haak, W. et al. 2008 Ancient DNA, Strontium isotopes, and osteological analyses shed light on social kinship organization of the later Stone Age. PNAS, vol. 105, no. 47:18226-18231.

25 Andersen, S. T. 1995 History of vegetation and agriculture at Hassing House Mose, Thy, northwest Denmark. *Journal of Danish Archaeology* 1992–1993: 39–57.

26 Kremenetski, K. 2003 Steppe and forest steppe belt of Eurasia: Holocene environmental history. In: *Prehistoric Steppe Adaptations and the Horse*, edited by M. Levine, C. Renfrew and K. Boyle, pp. 11–29. McDonald Institute Monographs, Cambridge.

27 Odgaard, B. V. 1994 The Holocene vegetation history of northern West Jutland, Denmark. *Opera Botanica* 123: 1–171.

28 Paschkevych, G. 2012 Environment and economic activities of Neolithic and Bronze Age populations of the Northern Pontic Area. *Quaternary International* 261:176-182.

29 Harrisson, R. and Heyd, V. 2007. The transformation of Europe in the third millennium BC: the example of 'Le Petit Chasseur I+III' (Sion, Valais, Sweitzerland). *Praehistorische Zeitschrift*, 82,129–214.

30 Heyd, V. 2007. Families, prestige goods, warriors and complex societies: Beaker groups and the 3rd millennium cal BC. *Proceedings of the Prehistoric Society*, 73, 327–381.

31 Heyd, V. 2011. Yamnaya groups and tumuli west of the Black Sea. In S. Müller Celka and E. Borgna (eds), *Ancestral landscapes: burial mounds in the Copper and Bronze Ages,* 535–555. Lyon: Maison de l'Orient et de la Mediterranée.

32 Kristiansen, K 1989. Prehistoric migrations—the case of the Single Grave and Corded Ware cultures. *Journal of Danish Archaeology* 8: 211-225.

33 Neustupny, E. 2013 The Prehistory of Bohemia. The Eneolithic. Praha.

34 Fuhrholt, M. 2011 Materieller Kultur und räumliche Strukturen sozialer Identität im 4. Und 3. Jt. V. Chr. In Mitteleuropa. Eine methodische Skizze. In S. Hansen, S. and Müller, J. (eds*.) Sozialarchäologische Perspektiven: Gesellschaftlicher Wandel 5000-1500 v. Chr. Zwischen Atlantik und Kaukasus*:243-267. Archäologie in Eurasien Band 24. Verlag Phillip von Zabern. Berlin.

35 Gerling, C. et al. 2012 Immigration and transhumance in the Early Bronze Age Carpathian Basin: the occupants of a kurga*n*. *Antiquity* 86:1097-1111.

36 Irrgeher, J., M. Teschler-Nicola, K. Leutgeb, C. Weiss, D. Kern and T. Prohaska 2012 Migration and mobility in the latest Neolithic of the Traisen Valley, Lower Austria: Sr isotope analysis. In E. Kaiser, J. Burger and W. Schier (eds.): *Population Dynamics in Prehistory and Early History.* New Approaches using stable isotopes and genetics:199-211. Topoi Berlin Studies of the Ancient World. De Gruyter, Berlin.

37 De Jong, H., Foster, G.L., Heyd, V., and Pike, A.W.G. 2010. Further Sr isotope studies

on the Eulau multiple graves using laser ablation ICP-MS. In H. Meller and K.W. Alt (eds), *Anthropologie, Isotopie und DNA—biographische Annäherung an Namenlose vorgeschichtliche Skelette?* 2. Mitteldeutscher Archäologentagung vom 8. Bis 10 oktober 2009 in Halle (Saale), 63–70. Halle: Landesamt für Denkmalpflege und Archäologie—Landesmuseum für Vorgeschichte.

38 Müller, J. et al 2009 A Revision of Corded Ware Settlement Pattern – New Results from the Central European Low Mountain Range. *Proceedings of the Prehistoric Society* 75: 125-142.

39 Koryakova, L. and A. Epimakhov 2007 *The Urals and Western Siberia in the Bronze and Iron Ages.* Cambridge University Press.

40 Kuznetsov, P. F. 2006 The emergence of Bronze Age chariots in eastern Europe. *Antiquity* 80: 638–645.

41 Krause, R. and L. Koryakova (eds.) 2013 *Multidisciplinary investigations of the Bronze Age settlements in the Southern Trans-Urals (Russia).* Frankfurter Archäologische Schriften 23. Habelt-Verlag. Bonn.

42 Krause, R. and L. Koryakova (eds.) 2014 *Zwischen Tradition ud Innovation. Studien zur Bronzezeit im Trans-Ural.* Frankfurter Archäologische Schriften 26. Habelt-Verlag. Bonn.

43 Grigoriev, S. A. 2002 *Ancient Indo-Europeans.* Charoid publishers: Sverdlovsk.

44 Kuzmina, E. 2007 The origin of the Indo-Iranians. Leiden: Brill.

45 Bendezu-Sarmiento, J. 2007 *De l'Âge du Bronze et lÂge du Fer au Kazakkstan, gestes funéraires et paramètres biologiques*. Identités culturelles des population Andronovo et Saka. De Boccard: Paris.

46 Kristiansen, K. 2011. Bridging India and Scandinavia. Institutional Transmission and Elite Conquest during the Bronze Age. In T. C. Wilkinson, S. Sherratt and J. Bennett (eds.): *Interweaving Worlds*. Systemic Interaction in Eurasia, 7th to the 1st Millennia BC: 243-265. Oxford: Oxbow Books.

47 Kristiansen, K. 2012 The Bronze Age expansion of Indo-European languages: an archaeological model. In C. Prescott and H. Glørstad (eds.): *Becoming European*. The transformation of third millennium Northern and Western Europé: 165-181. Oxbow Books:Oxford.

48 Legrand, S 2010 La *culture de Karasuk: définition de la société de l'Age du Bronze final dans le bassin de Minusinsk* (région du Moyen-Enisej, Sibérie méridionale). Paris.

49 Desideri, J. 2011. *When Beakers met Bell Beakers. An analysis of dental remains.* Oxford: British Archaeological Reports International Series 2292.

50 Price, D., Knipper, C., Grupe, G. & Smrcka, V. 2004. Strontium Isotopes and Prehistoric Human Migrations: The Bell Beaker Period in Central Europe. *European Journal of Archaeology* 7(1):9–40.

51 Vander Linden, M. 2012. Demography and mobility in north-western Europe during the third millennium BC. In C. Prescott and H. Glörstad (eds), *Becoming European. The transformation of third millennium northern and western Europe*, 19–29. Oxford: Oxbow Books.

52 Needham, S. 2005. Transforming Beaker culture in north-west Europe; processes of fusion and fission. *Proceedings of the Prehistoric Society*, 71, 171–217.

53 Fokkens, H. and Nicolis, F. (eds) 2012. *Background to Beakers*. Inquiries into regional cultural backgrounds of the Bell Beaker complex. Leiden: Sidestone Press.

54 Pokutta, D. 2013 *Population Dynamics, Diet and Migrations of the Unetice Culture in Poland.* University of Gothenburg. Gothenburg.

55 Müller, J. 2013 Demographic traces of technological innovation, social change and mobility: from 1 to 8 million Europeans (6000-2000 BCE). In S. Kadrow and P. Włodarczak (eds.*), Environment and subsistence – forty years after Janusz Kruk's*

„Settlement studies" (= Studien zur Archäologie in Ostmitteleuropa / Studia nad Pradziejami Europy Środkowej 11). Rzesz.w, Bonn: Mitel & Verlag Dr. Rudolf Habelt GmbH, 1–14.

56 Kristiansen, K. and T.B. Larsson, 2005. *The Rise of Bronze Age Society*. *Travels, Transmissions and Transformations.* Cambridge.

57 Wahl, J. and T.D. Price, 2013. 'Local and foreign males in a Late Bronze Age cemetery at Neckarsuhm, southwestern Germany: strontium isotope investigations', *Anthropologischer Anzeiger* 70(3), 289-307.

58 Earle, T. 2002. *Bronze Age Economics*. The Beginnings of Political Economies. Westview.

59 Demoule, J.-P. 2014 *Mais où sont passes les indo-Européens*? Le mythe d'origine de l'occident. Editions du Seuil. Paris.

60 Dergachev, V. 2000 The Migration theory of Marija Gimbutas. *Journal of Indo-European Studies*, Vol. 28, No. 3-4:257-319.

Section 2

Brief description of the samples

Details of the sampled individuals, locations and time periods are given in Supplementary Tables 1, 2, and 3, respectively. We have focused mainly on sampling human remains dating from the third and early to mid-second millennia BC. In cultural terms this corresponds to the period from Corded Ware/Yamnaya into the full European Bronze Age. The geographical cover is broad, stretching from Scandinavia, Central and Southern Europe over Eastern Europe, Southern Ural to Central Siberia (Fig 1, main text).

In all, 603 human samples were screened for ancient DNA (aDNA) preservation, of which 101 individuals were selected for deeper sequencing. The samples were in most cases teeth, preferably molars, although in a few cases also bone samples were used. Several criteria were applied when initially selecting samples; bone preservation as judged from visual inspection was a primary concern, but also archaeological relevance, quality of context and documentation was considered. Osteological analyses of the bones were performed specifically for the project on Scandinavian material. These were made by Lise Harvig on Danish material and by Torbjörn Ahlström for Swedish material. For other regions existing osteological analyses have been used.

More than 400 ^{14}C-dates are now available for the original set of 603 samples. ^{14}C-determinations of the selected subset are included, with calibrations (2 sigma) in Supplementary Table 1. It should be noted that the calibrations have been made without taking possible marine reservoir effects into account. Judging from the ^{13}C collagen values, this is likely to only affect one case, namely sample RISE61, from Kyndeløse in Denmark. It is a young man with a high marine signal, and his dating should likely be reduced by a couple of hundred years. Freshwater reservoir effects, as can be deduced from combined ^{13}C and ^{15}N values, are also of marginal importance in these data. The clearest exception could be three dates from Bulanovo in Russia, classified as Sintashta culture, which have raised ^{15}N values and also somewhat earlier dates than other Sintashta samples.

For the purpose of this paper, our ^{14}C dates have been used mainly as a check on contextual dating based on the archaeology, but also to date samples with a less clear cultural context. In most cases, ^{14}C dating and archaeological dating show a very good match, lending also more confidence to the contextual dating of those samples that are not yet ^{14}C dated.

Supplementary Table 1: Sample information (next page)

Details of all 101 individuals (102 samples) included in this project. RISE507 and RISE508 proved genetically identical and an evaluation of the museum catalogue confirmed that the two samples were from the same individual. *Sample* refers to internal sample numbers given by "The RISE" project. *Site* is the name of the locality where the skeleton was found. More details on the sites (lat-long coordinates etc) are found in Supplementary Table 2. *Culture or Age* refers to the cultural context of the sample as described above. *Sample info* refers to the particular burial and/or designations given by the excavators. *Sample type* indicates if it is a bone or tooth sample. We also list the available ^{14}C dates, along with calibrated dates (2 sigma). Osteological determinations of sex and age are listed, along with sex determinations based on DNA (see Section 5). Overall, there is a 75% agreement between the two methods of sex determination.

Supplementary Table 1: Sample information

Sample	Country	Site	Culture or Age	Sample info	Material	14C lab #	14C date, BP	Sta	cal BC low	cal BC high	Sex	DNA sex	Age class
RISE00	Estonia	Sope	Corded Ware	grave	tooth						F	F	Adult
RISE1	Poland	Oblaczkowo	Corded Ware	E8-A	tooth	UBA-16633	4117	28	-2865	-2578	nd	M	Infant
RISE21	Denmark	Karlstrup	Nordic BA	barrow 4 central grave, N skeleton #1	tooth	OxA-28047	3092	29	-1426	-1281	nd	M	Adult
RISE42	Denmark	Marbjerg	Nordic LN	PMD 98, III	tooth	OxA-28225	3681	28	-2191	-1972	M	M	Adult
RISE47	Denmark	Sebber skole	Nordic BA	N 358 grave 3 skeleton 8	tooth	OxA-28258	3153	26	-1499	-1324	M	M	Adult
RISE61	Denmark	Kyndelöse	Nordic MN B	PMD 17, V, N chamber lower layer	tooth	OxA-28296	4071	27	-2851	-2492	F	M	Adult
RISE71	Denmark	Falshöj	Nordic LN	PMD 57, I	tooth	OxA-28269	3701	26	-2196	-2023	M	F	Adult
RISE94	Sweden	Viby	Battle Axe	grave 26:I	tooth	OxA-29033	4025	30	-2621	-2472	M	M	Adult
RISE97	Sweden	Fredriksberg	Nordic LN	grave 72(II)	tooth	OxA-28986	3590	29	-2025	-1885	M	F	Adult
RISE98	Sweden	L Beddinge 56	Battle Axe/Nordic LN	grave 49, S skeleton	tooth	OxA-28987	3736	32	-2275	-2032	M	M	Adult
RISE109	Poland	Wojkowice	Unetice	grave 1044	tooth	UB-16557	3544	26	-1954	-1772	F	F	Adult
RISE139	Poland	Chociwel	Unetice	grave 20/2011	tooth	Ua-44034	3645	33	-2135	-1923	F	M	Adult
RISE145	Poland	Polwica	Unetice	grave 1603	tooth	UB-16564	3677	31	-2188	-1958	M	F	Adult
RISE150	Poland	Przeclawice	Unetice	grave 02	bone	Ua-42401	3469	31	-1885	-1693	M	F	Adult
RISE154	Poland	Szczepankowice	Unetice	grave 3	tooth	Uba-16555	3522	24	-1925	-1765	F	F	Adult
RISE174	Sweden	Oxie 7	Iron Age	grave 73	tooth	UBA-28275	1521	38	427 AD	611 AD	F	M	Adult
RISE175	Sweden	Abekås I	Nordic BA	barrow I grave 14:1	tooth	OxA-28998	3025	30	-1395	-1132	M	M	Adult
RISE179	Sweden	Abekås I	Nordic LN	barrow I grave 5:1, gallery grave	tooth	OxA-29193	3556	28	-2010	-1776	M	M	Adult
RISE207	Sweden	Ängamöllan	Nordic BA	Cranium XII	tooth	OxA-29651	3130	27	-1493	-1302	nd	M	Infant
RISE210	Sweden	Ängamöllan	Nordic BA	Cranium VI	tooth	OxA-29654	3105	28	-1432	-1292	M	F	Adult
RISE240	Russia	Sukhaya Termista I	Yamnaya	kurgan 1, grave 11	tooth	GrA-45038	4160	30	-2880	-2632	F	F	Adult
RISE247	Hungary	Százhalombatta-Földvár	Vatya	ID 3437	bone	OxA-29769	3372	29	-1746	-1611	nd	M	nd
RISE254	Hungary	Százhalombatta-Földvár	Vatya	ID 4091	bone	OxA-29842	3631	29	-2128	-1909	nd	M	nd
RISE276	Denmark	Trundholm mose II	Nordic LBA	bog find 1940	tooth	OxA-30485	2525	25	-794	-547	M	M	Adult
RISE349	Hungary	Battonya Vörös Oktober	MBA	Grave # 33	tooth	OxA-30987	3588	34	-2034	-1784	F	F	Adult
RISE371	Hungary	Szöreg - C (Sziv Utca)	Maros	Grave # 105	tooth	OxA-30988	3653	32	-2136	-1941	F	F	Adult
RISE373	Hungary	Szöreg - C (Sziv Utca)	Maros	Grave # 123	tooth	OxA-31104	3476	30	-1886	-1696	F	F	Adult
RISE374	Hungary	Szöreg - C (Sziv Utca)	Maros	Grave # 147	tooth	OxA-30989	3402	34	-1866	-1619	M	M	Adult
RISE386	Russia	Bulanovo	Sintashta	burial 4	tooth	OxA-30991	3775	34	-2298	-2045	M	M	Adult
RISE391	Kazakhstan	Tanabergen II	Sintashta	kurgan 7 burial 36	tooth	OxA-30998	3612	34	-2120	-1887	M	F	Adult
RISE392	Russia	Stepnoe VII	Sintashta	kurgan 4 burial B	tooth	OxA-30999	3626	33	-2126	-1896	M	M	nd
RISE394	Russia	Bulanovo	Sintashta	burial 6 skeleton 1	tooth	OxA-30993	3532	34	-1949	-1754	F	F	Adult
RISE395	Russia	Bol'shekaraganskii	Sintashta	kurgan 25 burial 12	tooth	OxA-30996	3540	33	-1960	-1756	F	F	Adult
RISE396	Armenia	Kapan	LBA	tomb 6 skeleton 1	tooth	OxA-31001	2879	31	-1192	-937	F	F	Adult
RISE397	Armenia	Kapan	LBA	tomb 6 skeleton 2	tooth	OxA-31002	2807	31	-1048	-855	F	M	Juv
RISE407	Armenia	Norabak	LBA	#5	tooth	UBA-27938	2827	40	-1115	-895	nd	F	Infant
RISE408	Armenia	Norabak	LBA	#6	tooth	UBA-27939	2908	32	-1209	-1009	F	M	Adult
RISE412	Armenia	Noratus	LBA	#10	tooth	UBA-27940	2885	31	-1193	-945	F	F	Adult
RISE413	Armenia	Nerquin Getashen	MBA	#11	tooth	UBA-28941	3493	34	-1906	-1698	M	M	Adult
RISE416	Armenia	Nerquin Getashen	MBA	#14	tooth	UBA-27942	3259	40	-1643	1445	nd	M	Infant
RISE423	Armenia	Nerquin Getashen	MBA	#21	tooth	UBA-27944	3038	32	-1402	-1211	M	M	Adult
RISE431	Poland	Leki Male	Corded Ware/proto-Unetice	Barrow 4, skeleton 2	tooth	OxA-27967	3762	27	-2286	-2048	M	M	Adult

RISE434	Germany	Tiefbrunn	Corded Ware	3/1	tooth	UBA-27946	4161	34	-2880	-2630	F	M	Adult
RISE435	Germany	Tiefbrunn	Corded Ware	3/2	tooth	UBA-27947	4094	33	-2863	-2498	nd	F	Infant
RISE436	Germany	Tiefbrunn	Corded Ware	3/3	tooth	UBA-27948	4124	31	-2868	-2580	M	M	Adult
RISE446	Germany	Bergrheinfeld	Corded Ware	burial 13 male	tooth	UBA-27950	4015	38	-2829	-2465	M	M	Adult
RISE471	Germany	Untermeitingen	BA	burial 1	tooth						M	nd	Adult
RISE479	Hungary	Erd 4	Vatya	ID 1129/1706 Q3 (P23)	bone						nd	M	Juvenile
RISE480	Hungary	Erd 4	Vatya	ID 1039/1550 Q1 (P24)	bone						nd	F	Adult
RISE483	Hungary	Erd 4	Vatya	ID 106/159 Q2 (P27)	bone						nd	F	Adult
RISE484	Hungary	Erd 4	Vatya	ID 772/1170 Q3 (P28)	bone						nd	F	Infant
RISE486	Italy	Remedello di Sotto	Remedello	T78	tooth	ETH-12913	3595	55	-2134	-1773	M	M	Adult
RISE487	Italy	Remedello di Sotto	Remedello	T56	tooth	OxA-X-2621	4557	28	-3483	-3107	nd	M	Juvenile
RISE489	Italy	Remedello di Sotto	Remedello	T65	tooth	ETH-12188	4185	70	-2908	-2578	M	M	Adult
RISE492	Russia	Sabinka 2	Iron Age	7332-6	tooth	OxA-31210	2257	27	-396	-209	M	M	Adult
RISE493	Russia	Sabinka 2	Karasuk	7332-45	tooth	OxA-31211	3214	26	-1531	-1427	M	M	Adult
RISE494	Russia	Sabinka 2	Karasuk	7332-35	tooth	OxA-31212	3081	27	-1416	-1268	M	M	Adult
RISE495	Russia	Arban 1	Karasuk	7332-175	tooth						M	M	Adult
RISE496	Russia	Arban 1	Karasuk	7332-172	tooth	OxA-31213	3070	28	-1414	-1261	F	F	Adult
RISE497	Russia	Arban 1	Karasuk	7332-188	tooth						M	F	Adult
RISE499	Russia	Bystrovka	Karasuk	5909-5	tooth						F	F	Adult
RISE500	Russia	Kytmanovo	Andronovo	6652-38	tooth						F	F	Adult
RISE502	Russia	Bystrovka	Karasuk	5909-4	tooth	OxA-31214	3140	27	-1496	-1306	F	F	Adult
RISE503	Russia	Kytmanovo	Andronovo	6652-41	tooth	OxA-31445	3328	38	-1727	-1511	M	F	Adult
RISE504	Russia	Kytmanovo	Iron Age	6652-35	tooth	OxA-31215	1208	24	721 AD	889 AD	F	M	Adult
RISE505	Russia	Kytmanovo	Andronovo	6652-42	tooth	OxA-31216	3391	27	-1746	-1626	M	F	Adult
RISE507*	Russia	River Kuyum	Afanasievo	5910-2A	tooth	OxA-31219	4423	29	-3322	-2923	nd	F	nd
RISE508*	Russia	River Kuyum	Afanasievo	5910-2B	tooth	OxA-31220	4442	29	-3331	-2935	nd	F	nd
RISE509	Russia	Bateni	Afanasievo	6136-5	tooth	OxA-31221	4186	27	-2887	-2677	F	F	Adult
RISE510	Russia	Bateni	Afanasievo	6136-9	tooth	OxA-31222	4040	45	-2851	-2468	F	F	Adult
RISE511	Russia	Bateni	Afanasievo	6136-6	tooth	OxA-31568	4224	36	-2909	-2679	F	F	Adult
RISE512	Russia	Kytmanovo	Andronovo	6652-39	tooth	OxA-31217	3119	27	-1446	-1298	M	M	Adult
RISE515	Russia	Verkhni Askiz Village	Okunevo	7053-1	bone	UCIAMS-147669	3810	25	-2340	-2145	F	F	Adult
RISE516	Russia	Verkhni Askiz Village	Okunevo	7053-2	bone	UCIAMS-147668	3725	25	-2201	-2036	F	F	Adult
RISE523	Russia	Kapova cave	Mezhovskaya	Square E-7, N:14 (-26.5 cm), 2011	tooth	OxA-31447	3192	37	-1598	-1398	nd	F	nd
RISE524	Russia	Kapova cave	Mezhovskaya	Square E-7, N:25, southern sector	tooth						nd	M	nd
RISE525	Russia	Kapova cave	Mezhovskaya	Square R-8, depth -4/-10	skull						nd	M	nd
RISE546	Russia	Temrta IV	Yamnaya	Kurgan 1, grave 13	tooth						M	M	Juvenile
RISE547	Russia	Temrta IV	Yamnaya	Kurgan 1, grave 9	tooth	GrA-58960	4175	35	-2887	-2634	M	M	Adult
RISE548	Russia	Temrta IV	Yamnaya	Kurgan 1, grave 6	tooth						M	M	Adult
RISE550	Russia	Peshany V	Yamnaya	Kurgan 1, grave 3	tooth	IGAN-2880	4312	94	-3334	-2635	M	M	Adult
RISE552	Russia	Ulan IV	Yamnaya	Kurgan 4, grave 8	tooth	IGAN-4079	3940	90	-2849	-2143	M	M	Adult
RISE553	Russia	Afontova Gora	LBA	CGG_2_011881	bone	OxA-31140	2731	28	-926	-815	nd	M	nd
RISE554	Russia	Afontova Gora	LBA	CGG_2_011884	bone	OxA-31141	2782	30	-1005	-844	nd	M	nd
RISE555	Russia	Stalingrad Quarry	EBA	CGG_2_011887	tooth	AAR-20358	4082	28	-2857	-2497	nd	M	nd
RISE559	Germany	Augsburg	Bell Beaker	F0174, gr 4	tooth						F	F	Adult
RISE560	Germany	Augsburg	Bell Beaker	F0187, gr 3	tooth						M	M	Adult
RISE562	Germany	Landau an der Isar	Bell Beaker	F0228, obj. 136/92 = gr.9	tooth						F	F	Adult
RISE563	Germany	Osterhofen-Altenmarkt	Bell Beaker	F0234, obj. 8	tooth						M	M	Adult

RISE564	Germany	Osterhofen-Altenmarkt	Bell Beaker	F0241, obj. 25	tooth						M	M	Adult
RISE566	Czech Republic	Knezeves	Bell Beaker	F0521, A01168, gr. 14	tooth						M	M	Infant
RISE567	Czech Republic	Knezeves	Bell Beaker	F0523, A0766, gr. 8	tooth						M	F	Adult
RISE568	Czech Republic	Brandysek	Bell Beaker	F0525, A01623, gr. 16	tooth						nd	F	Infant
RISE569	Czech Republic	Brandysek	Bell Beaker	F0527, A01643, gr. 35?	tooth						nd	F	Infant
RISE577	Czech Republic	Velke Prilepy	Unetice	F0565, gr. 238	tooth						M	F	Adult
RISE586	Czech Republic	Moravska Nova Ves	Unetice	F0597, gr. 6	tooth						F	F	Adult
RISE595	Montenegro	Velika Gruda	LBA	Grave 3	tooth						M	F	Adult
RISE596	Montenegro	Velika Gruda	Iron Age	Grave 36	tooth						F	F	Adult
RISE598	Lithuania	Turlojiske	LBA	1755, bog find	bone	Ua-16681	2590	75	-908	-485	M	M	Adult
RISE600	Russia	Verh-Uimon	Iron Age	13-1, grave 20	tooth						M	M	Adult
RISE601	Russia	Verh-Uimon	Iron Age	18-1, grave 35	tooth						M	M	Adult
RISE602	Russia	Sary-Bel	Iron Age	23-1, grave 2	tooth						nd	M	Adult

* Same individual

Supplementary Table 2: Site information

The table includes country, site name, site type, lat/long coordinates, and archaeological period/culture. Note that some sites are multi-phase, so the site dating is in many cases wider than the date of individual samples in Supplementary Table 1. Note also that period names are used differently in different areas and the same period name may refer to different absolute ages. BBC=Bell Beaker Culture, CWC= Corded Ware Culture, MN=Middle Neolithic, LN=Late Neolithic, EBA=Early Bronze Age, MBA=Middle Bronze Age, LBA=Late Bronze Age, BA=Bronze Age, IA=Iron Age, nd= no data.

Country	Site name	Site type	Site period or culture	Longitude	Latitude
Armenia	Kapan	grave	LBA	46,4	39,2
Armenia	Nerquin Getashen	grave	MBA	45,26	40,14
Armenia	Norabak	grave	LBA	45,86	40,15
Armenia	Noratus	grave	LBA	45,18	40,38
Czech Republic	Brandysek	cemetery	BBC	14,158	50,19
Czech Republic	Knezeves	cemetery	BBC	14,258	50,118
Czech Republic	Moravska Nova Ves	cemetery	Unetice	17,022	48,799
Czech Republic	Velke Prilepy	cemetery	Unetice	14,311	50,16
Denmark	Falshöj	megalithic tomb	Nordic LN	10,034	56,676
Denmark	Karlstrup	barrow	Nordic EBA	12,209	55,55
Denmark	Kyndelöse	passage grave	Nordic MN	11,855	55,703
Denmark	Marbjerg	gallery grave	Nordic LN	12,148	55,657
Denmark	Sebber skole	flat graves	Nordic EBA	9,552	56,97
Denmark	Trundholm mose II	bog find	Nordic LBA	11,565	55,914
Estonia	Sope	grave	CWC	27,026	59,408
Germany	Augsburg	cemetery	BBC	10,895	48,33
Germany	Bergrheinfeld	cemetery	CWC	10,18	50,009
Germany	Landau an der Isar	cemetery	BBC	12,707	48,663
Germany	Osterhofen-Altenmarkt	cemetery	BBC	13,016	48,691
Germany	Tiefbrunn	grave	CWC	12,259	48,932
Germany	Untermeitingen	barrow	MBA	10,814	48,17
Hungary	Battonya Vörös Oktober	cemetery	MBA	20,985	46,356
Hungary	Erd 4	settlement	Vatya, MBA	18,896	47,341
Hungary	Százhalombatta-Földvár	tell	Vatya, MBA	18,962	47,327
Hungary	Szöreg - C (Sziv Utca)	cemetery	Maros, MBA	20,199	46,22
Italy	Remedello di sotto	cemetery	Copper Age	10,379	45,26
Kazakhstan	Tanabergen II	kurgan	Sintashta	56,83	50,593
Lithuania	Turlojiske	bog find	LBA	23,302	54,358
Montenegro	Velika Gruda	barrow	LBA-IA	18,74	42,382
Poland	Chociwel	cemetery	Unetice	17,094	50,796
Poland	Leki Male	cemetery, barrow	CWC/proto-Unetice	16,538	52,143
Poland	Oblaczkowo	grave	CWC	17,54	52,29
Poland	Polwica	cemetery	Unetice	17,177	50,913
Poland	Przeclawice	cemetery	Unetice	16,957	50,918
Poland	Szczepankowice	barrows	Unetice	16,943	50,948
Poland	Wojkowice	cemetery	Unetice	17,068	50,98
Russia	Afontova Gora	grave	LBA-IA	92,866	56,016
Russia	Arban 1	grave	Karasuk, BA	90,187	52,954
Russia	Bateni	grave	Afanasievo, BA	90,775	54,584
Russia	Bol'shekaraganskii	kurgan	Sintashta	59,536	52,637
Russia	Bulanovo	cemetery	Sintashta	55,16	52,453
Russia	Bystrovka	grave	Karasuk, LBA	88,574	51,909
Russia	Kam-Tyttugem	rock shelter	IA	89,003	49,923
Russia	Kapova cave	cave	Meshovskaya, LBA	57,066	53,043
Russia	Kytmanovo	grave	Andronovo, BA + IA	85,447	53,456
Russia	Peshany V	Kurgan	Yamnaya	43,676	46,556
Russia	River Kuyum	grave	Afanasievo, BA	85,97	51,498
Russia	Sabinka 2	grave	Karasuk, BA	91,05	53,152
Russia	Sary-Bel	kurgan	IA	86,459	50,615
Russia	Stalingrad Quarry	burial	BA	44,5	48,716
Russia	Stepnoe VII	kurgan	Sintashta	59,076	53,876
Russia	Sukhaya Termista I	Kurgan	Yamnaya	43,678	46,58
Russia	Temrta IV	kurgan	Yamnaya	43,699	46,539
Russia	Ulan IV	Kurgan	Yamnaya	43,334	46,615
Russia	Verh-Uimon	kurgan	IA	85,725	50,213
Russia	Verkhni Askiz Village	grave	Okuneva, BA	90,194	53,153
Russia	Zhana-Aul	kurgan	IA	88,668	49,995
Sweden	Abekås I	Barrow	Nordic LN-EBA	13,6	55,397
Sweden	Fredriksberg	flat graves	Nordic LN	13,059	55,557
Sweden	L Beddinge 56	flat graves	BAC/LN	13,445	55,381
Sweden	Oxie 7	flat grave	IA	13,098	55,545
Sweden	Snorthög	Barrow + flat graves	BAC/LN	13,291	55,494
Sweden	Viby	flat graves	BAC	14,233	56,025
Sweden	Ängamöllan	gallery grave	Nordic EBA	14,104	55,997

Supplementary Table 3: Summary of chronological overview of the cultures and periods discussed in Section 1. MN B=Middle Neolithic B, LN=Late Neolithic, EBA=Early Bronze Age. BC cal = estimated calibrated age span of the period.

Culture	BC cal
Majkop	3700-3000
Remedello 1	3400-2800
Afanasievo	2900-2500
Yamnaya	3000-2400
Catakomb	2800-2200
Corded Ware	2800-2300
Single Grave	2800-2300
Battle Axe	2800-2300
Nordic MN B	2800-2200
Bell Beaker	2600-2000
Okunevo	2500-2000
Unetice	2300-1800
Maros	2300-1500
Sintashta	2100-1800
Nordic LN	2200-1800
Vatya	2000-1500
Nordic EBA	1800-1150
Andronovo	1700-1500
Karasuk	1400-900
Mezhovskaya	1300-800/700
Iron Age	9/700 BC-AD 500/1000

Section 3

Laboratory work and sample selection

3.1 The samples

A total of 603 human Bronze Age samples from across Europe were selected for the initial molecular 'screening' to assess the DNA preservation and hence the potential for genome-scale analyses. The samples consisted almost exclusively of teeth, but also a few bone and hair samples were included. Five hair samples, DNA extracted as in[1] did not yield any positive results according to our three threshold criteria (see Section 3.4), and the following descriptions relates only to the teeth and bone samples.

3.2 Ancient DNA extraction with new improvements

All the molecular work (pre-library amplification) was conducted in dedicated aDNA clean lab facilities at Centre for GeoGenetics, Natural History Museum, University of Copenhagen, using strict aDNA guidelines[2,3]. The lab work described spanned a considerable period of time and, in particular, the DNA extraction methods were continually assessed and optimized. As a result, the samples were not all processed in the exact same manner but by some combination of the protocols outlined below.

To minimize potential contamination from modern DNA due to previous handling, the surface of the tooth or bone was first removed using the edge of a diamond-dust-coated cutting disk with a mechanical drill. The crown of the tooth was separated from the root using another cutting disk. For the majority of teeth we then used a pointy drill-bit to sample the inner layers of the roots (the dentine) but as the work progressed, we realized that we obtained much better results (i.e. a higher fraction of DNA sequences identified as human) when extracting from the outer cementum layer instead of the dentine. This sampling method is described in detail elsewhere[4]. The amount of starting material varied but was generally 100-600 mg.

A second improvement involved the inclusion of a 'pre-digestion' step, where the drilled bone or tooth powder is incubated in digestion buffer for 15-30 minutes prior to the 24h full digestion step. This treatment facilitates the removal of surface contaminants and hence results in a higher proportion of endogenous DNA in the final extract. The details are described elsewhere[4].

Whether pre-digested or not, the drilled or crushed material was incubated for 24 hours at 45 ºC in 5 ml digestion buffer containing 4.7 ml 0.5 M EDTA, 50 µL Proteinase K (0.14-0.22 mg/ml, Roche) and 250 µL 10% N-Laurylsarcosyl. Following incubation the samples were spun down and pellets were stored for later re-extraction. A silica-powder-based extraction method [5,6] was used to isolate the DNA from the supernatant. The silica suspension was prepared by mixing 6g of SiO_2 with 50 ml sterile H_2O, followed by 1 hour of sedimentation.

48 ml supernatant was transfered to a 50 ml tube followed by another 5 hour sedimentation. Then the top 43 ml was carefully removed and the silica was resuspended and activated with 60 ul 37% HCL for use. For most of the samples we used a binding buffer that was prepared by mixing 118.2 g Guanidinium Thiocyanate with 10 mL Tris 1M, 1 mL NaCl 5M, 8mL EDTA 0.5M, 1 g N-Lauryl-Sarcosyl and molecular grade H_2O to a total volume of 200 ml. Then 20 mL of the binding buffer and 100 µl silica suspension was transferred to each sample and adjusted to pH 4-5 with 37% HCl. After a 3 hour incubation at room temperature the supernatant was removed and the pelleted silica was resuspended in 1 ml binding buffer and washed twice with 80% cold ethanol. Finally, the DNA was eluted in 60 µl EB buffer (Qiagen). Extraction blanks were included with each round of extractions.

An improved binding buffer

Specifically for this study, we developed a new binding buffer that proved highly efficient in recovering very short DNA fragments when initially tested on three ancient bone samples (Supplementary Figure 1). The buffer (pH = 4-5) was prepared in bulk by mixing 500 ml Qiagen buffer PB with 9 ml sodium acetate (5M), and 1.25 ml sodium chloride (5M). DNA extracts from ancient samples most often contain highly fragmented DNA (<200 bp) in addition to relatively long fragments (0.5 - >10 kb) which is modern non-target DNA, such as that from microorganisms living on the sample. Following the protocol by Rohland and Hofreiter [5], the recovery of short DNA fragments is relatively modest but by using our new binding buffer, we found a much-increased molarity of short DNA fragments as compared to total DNA recovery. We also tested our new PB-based binding buffer with the use of MinElute columns (Qiagen) with extension reservoirs for larger volumes as described elsewhere[7]. Supplementary Figure 1 shows representative results of comparison between the three methods of DNA binding. Samples were split in equal fractions after digestion for pairwise comparison. Our new buffer performed more efficiently at recovering short DNA fragments when applied with silica in solution rather than with MinElute columns (Supplementary Figure 1). The extraction with the new buffer were for most samples performed as described above, but we also tested larger volumes of binding buffer to digest buffer (as much as 10 to 1) and shorter silica-binding incubation times (1 hour), both of which appeared to increase the recovery of shorter fragments even more.

This general shift towards shorter DNA fragments with the new buffer is important because the ancient target DNA is often highly degraded and is therefore likely to constitute a larger proportion of the shorter DNA fragments than the longer fragments. It has been demonstrated that a shift towards shorter fragments can lead to a significant increase in the endogenous DNA content in the sequencing [7]. To initially test the efficiency of our new PB-based buffer we used Illumina shotgun sequencing (library preparation and bioinformatics as described below) on five ancient teeth extracted in parallel with the two different binding buffers. The sequencing results showed very clearly that our new PB-based buffer was much more efficient in recovering short fragments than the Guanidinium Thiocyanate binding buffer we had previously used, generally shifting from c. 90 bp average read length (after bioinformatic trimming, see below) to c. 55 bp (Supplementary Table 4). In three of the five cases this also

translated into a markedly higher human DNA content with up to 10-fold enrichment, whereas two samples performed moderately poorer with the new buffer (Supplementary Table 4).

Supplementary Figure 1: **Testing two binding buffers**

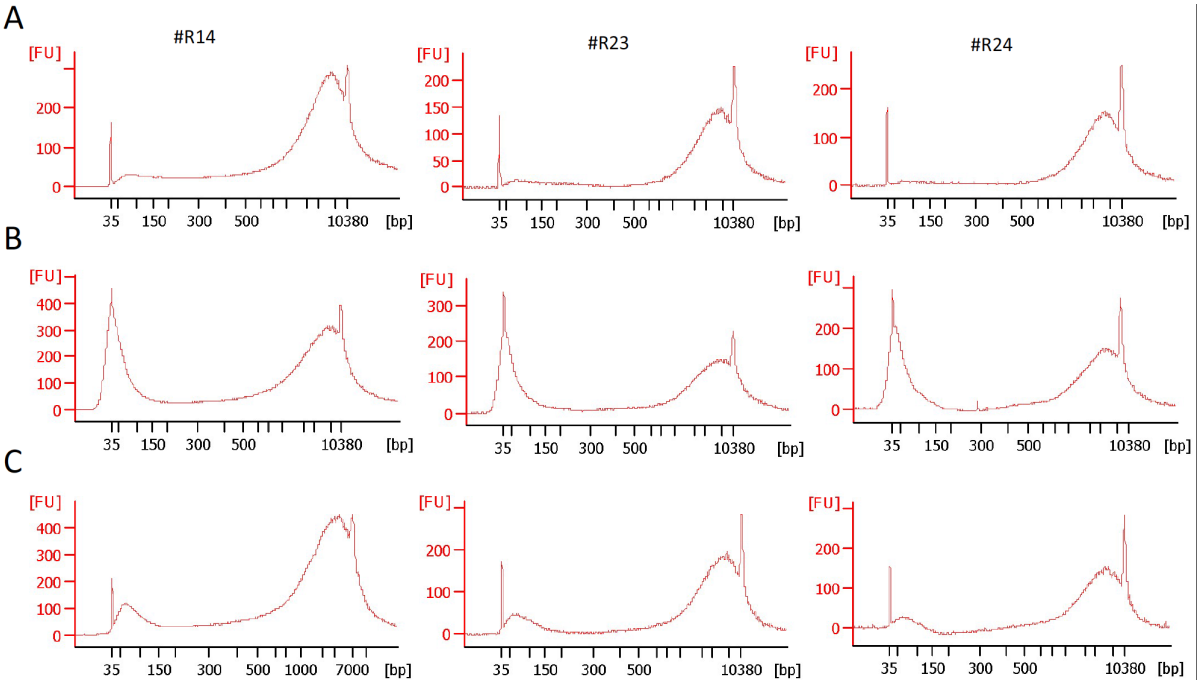

Length distributions of DNA extracted from ancient bone samples, analysed by BioAnalyzer (High Sensitivity). 300 mg of Bone powder from samples (R14, R23 and R24) were extracted in parallel using our traditional buffer (A), and using our new buffer developed for this study (B). We also tested our new buffer in combination with MinElute columns (Qiagen) with extension reservoirs as described elsewhere[7] (C). The size markers are seen as sharp peaks (at 35 bp and 10,380 bp). Our new buffer provides a large increase in molarity of short DNA fragments, in particular when applied with silica in solution (B) rather than columns (C). This is observed, in particular in panel B as a marked increase in short DNA fragments close to the 35 bp marker.

Although we have been observing an increased success rate in our lab after shifting to this new buffer, we note that it should be used cautiously. Applying this buffer can sometimes result in a large proportion of the sequencing reads being less than 30 bp long, which is about the critical length for reliable bioinformatic mapping. Also, a shift to shorter fragments will likely only have a significant positive effect if the target DNA is severely fragmented. If this is not the case, the benefits in shifting the fragment length distribution towards shorter fragments will likely be insignificant and could even result in overall lower genomic coverage after sequencing. As always with ancient DNA extractions there is a lot of variation in preservation among samples and further systematic experiments are needed to test the consistency of the improvement.

Our results suggest that there could be a benefit of splitting the sample (post-digestion) and then run two different extraction methods in parallel. This will increase the chance of obtaining at least one highly successful extract and also help identify the best method for that particular sample, which is relevant if more material is available.

Supplementary Table 4: Effects of two binding buffer on the DNA sequences

Sequencing and mapping statistics for the five ancient teeth that were DNA extracted with the two different binding buffers. The *A* extractions refer to the new PB-based binding buffer and *B* extractions were based on the 'traditional' Guanidinium Thiocyanate binding buffer. *Total* is the total number of DNA reads per extract, and *After trim,* is number sequences passing quality and length filtering. *Unique* is the number of sequences mapping uniquely to the human reference genome, and and *Rmdup* is the same number but with all duplicate sequences removed. *Human %* is the proportion of sequences after trimming that could identified as human, and *Clon %* is the proportion of identical reads (clones) in this human DNA fraction. *Efficiency* % is the overall library sequencing efficiency (*Rmdup/Total*). *Length*, shows the average length in basepairs of the DNA reads after trimming.

Sample #	Total	After trim	Unique	Rmdup	Clon %	Human %	Efficiency %	Length, bp
1A	14803410	10565224	1973979	1893301	4,1	18,7	12,8	47,6
1B	24184175	23928505	1589956	1522058	4,3	6,6	6,3	87,8
2A	15180456	13467493	6039106	5865516	2,9	44,8	38,6	52,2
2B	9896530	9592213	1122142	1009774	10,0	11,7	10,2	91,7
3A	12547183	11082931	3800370	3689011	2,9	34,3	29,4	55,1
3B	8056501	7556453	210966	195785	7,2	2,8	2,4	86,8
4A	54048658	49154837	8834466	8523839	3,5	18,0	15,8	58,1
4B	9477617	9204486	2221402	2113818	4,8	24,1	22,3	84,3
5A	23289218	19862232	1602618	779279	51,4	8,1	3,3	62,5
5B	8380122	7678194	922482	745969	19,1	12,0	8,9	96,1

The overall improvement

The average endogenous DNA content among the 115 best samples we screeened was 7.9% but there was a considerable difference between samples that had been treated with the traditional procedure (sampling dentine, no pre-digestion, traditional binding buffer) when compared to samples that were treated with the new improved methodology outlined above. The average endogenous DNA content among the samples with the traditional method was 3.8% (n = 71) whereas after switching to new methods we observed an almost 4-fold increase with an average endogenous DNA content of 14.5% (n = 44). This improvement cannot, however, serve as a formal test since the switch in methodology was continual and did not involve the same set of samples being treated with both methods in a comparative set up. However, the overall positive effects on our samples when switching to the new method seem unquestionable. More controlled experiments that document the positive impact of cementum sampling and pre-digestion are documented elsewhere[4].

3.3 Library preparation

Following extraction, 20 µl of DNA extract was built into a blunt-end library using the NEBNext DNA Sample Prep Master Mix Set 2 (E6070) and Illumina-specific adapters[8]. The libraries were prepared according to manufacturer's instructions, with a few modifications outlined below[6]. Because ancient DNA is already highly fragmented, the initial nebulization step was skipped. The end-repair step was performed in 25 µl reactions using 20 µl of DNA extract. This was incubated for 20 mins at 12°C and 15 mins at 37°C, and purified using PN buffer with Qiagen MinElute spin columns, and eluted in 15 µl. Next, Illumina-specific adapters (prepared as in[8]) were ligated to the end-repaired DNA in 25 µl reactions. The reaction was incubated for 15 mins at 20°C and purified with PB buffer on Qiagen MinElute columns, before eluted in 20 µl EB Buffer. The adapter fill-in reaction was performed in a final volume of 25 µl and incubated for 20 mins at 37°C followed by 20 mins at 80°C to inactivate the Bst enzyme. The entire DNA library (25 µl) was then amplified and indexed in a 50 µl PCR reaction, mixing with 5 µl 10X PCR buffer, 4 µl $MgCl_2$ (50 mM), 1 µl BSA (20 mg/ml), 0.5 µl dNTPs (25 mM), 1 µl of each primer (10 µM, inPE forward primer + indexed reverse primer), and 1 µl AmpliTaq Gold DNA Polymerase (Applied Biosystems). Thermocycling conditions were 5 min at 94°C, followed by 12 cycles of 30s at 94°C, 30s at 60°C and 40s at 72°C, and a final 7 min elongation step at 72°C. This was followed by a second PCR reaction (25 µl and 8 cycles) using 5 ul of the 'pre-amplified' library and P5/P7 primers[8]. The amplified library was purified with PB buffer on Qiagen MinElute columns, before being eluted in 30 µl EB. Negative library controls, constructed on H_2O, were included, as well as libraries constructed on the negative extractions controls.

3.4 Molecular screening and selection of candidate samples

All >600 aDNA libraries were 'shot-gun' sequenced in pools using Illumina HiSeq2500 platforms and 100bp single read chemistry. For the molecular screening phase we generally generated between 5 and 20 million reads per sample and these were used to evaluate the state of molecular preservation and hence the potential for obtaining genome-wide data. This selection of the candidate samples for further sequencing was based on fulfilling the following three requirements:

1) As a crude measure for the presence of authentic aDNA templates, the DNA library should display a >10% C-T misincorporation damage signal in the 5'- ends, when compared to the human reference genome (see Section 5 for more details).

2) Following bioinformatical filtering (Section 5), the fraction of DNA sequences that could be dentified as human should exceed 0.5%. For most ancient samples this human DNA fraction (the endogenous DNA) is extremely low making shotgun sequencing too inefficient for genome-scale profiling. It was therefore necessary to establish a cut-off value that somehow balanced research ambitions (in terms of sample size) with economic feasibility.

3) Following bioinformatical filtering, sequence clonality in the human DNA fraction should be less than 30%. In the downstream genomic analyses we are only interested in unique reads and libraries with high levels of clonality are therefore not suitable.

Based on these guidelines we selected 101 individuals for deeper sequencing. See Supplementary Table 1 and 2 for archaeological information on the samples and Supplementary Information Sections 5 for details on sequencing statistics and DNA damage.

3.5 Genomic capture

We selected 24 samples with relatively low human DNA content (0.5%-1.1%) for a whole genome capture experiment[9]. This was done to enrich for the low human DNA fraction in these samples. Prior to capture the 24 libraries were reamplified for between 3 and 14 cycles using primers IS5 (5'-AATGATACG GCGACCACCGA) and IS6 (5'-CAAGCAGAAGACGGCATACGA) and the same PCR set-up conditions as above to produce the 100-500 ng of total DNA required for capture. The capture was performed using the MYbait Human Whole Genome Capture Kit (MYcroarray, Ann Arbor, MI), following the manufacturer's instructions (http://www.mycroarray.com/pdf/MYbaits-manual.pdf). Post-capture, the libraries were amplified again for between 12 and 28 cycles using primers IS5 and IS6 and the same PCR set-up conditions as before. The optimal number of cycles for the post-capture amplification of each library was determined using qPCR. After amplification, the libraries were purified using Agencourt AMPure XP beads, quantified using an Agilent 2100 bioanalyzer, pooled in equimolar amounts, and sequenced on Illumina HiSeq 2000 as described above. The results are illustrated in Supplementary Table 5.

The capture experiment was highly successful in enriching the endogenous DNA content between 2.3 and 35.5 times (Supplementary Table 5). With a 13-fold average increase, this is comparable to what has been observed before[9,10]. However, it is also clear that the capture methodology causes a significant reduction in the molecular complexity in the library, resulting very high clonality among the reads, as previously observed[10]. Hence the gain in terms overall library efficiency (number of non duplicated reads per total reads) is more modest with these samples. We observe an average 2.6-fold increase in library efficiency following capture, but in four occasions the library efficiency is reduced with capture due to a dramatic increase in clonality (Supplementary Table 5). Also, as has been observed before the capture method introduces a skew in the DNA fragment length distribution resulting in slightly longer sequences post capture (overall average increase = 3.2 bp).

Supplementary Table 5: Genomic capture

Result of genomic capture experiment on 24 DNA libraries. *Total* is the total number of DNA reads per library, and *After trim,* is number sequences passing quality and length filtering. *Unique* and *Rmdup*, are number of sequences mapping uniquely to the human reference genome, and the same number but with all duplicate sequences removed, respectively. *Endo %* is the proportion of sequences after trimming that could be identified as human, and *Clon %* is the proportion of identical reads (clones) in this human DNA fraction. *Length change* is the increase in sequence lenght post capture. *Efficiency* % is the overall library sequencing efficiency (*Rmdup/Total*). *Fold improvements* are shown for the endogenous content and the efficiency for each captured library and overall.

										Capture improvement	
Sample #	Total	After trimming	Unique	Rmdup	Clon %	Endo %	Av. length of trimmed	Length change, bp	Efficiency %	Fold endo	Fold efficiency
MA182_L1	12394738	11828617	64269	55285	14,0	0,5	68,0		0,4		
MA182_L1_CAP	28039519	27452352	4872733	347467	92,9	17,7	74,3	6,3	1,2	32,7	2,8
MA203_L1	6672304	4922027	33964	33208	2,2	0,7	53,8		0,5		
MA203_L1_CAP	37593849	34013707	3723175	1397359	62,5	10,9	60,0	6,2	3,7	15,9	7,5
MA214_L1	34801898	34658318	241733	240219	0,6	0,7	53,0		0,7		
MA214_L1_CAP	33669403	33142445	3150596	2622861	16,8	9,5	58,1	5,1	7,8	13,6	11,3
MA294_L1	12214962	10967852	98781	96220	2,6	0,9	52,4		0,8		
MA294_L1_CAP	42163448	39969126	3855201	1376914	64,3	9,6	56,0	3,6	3,3	10,7	4,1
MA321_L1	24130329	17699822	106578	90798	14,8	0,6	70,0		0,4		
MA321_L1_CAP	50876395	44776982	9558905	358146	96,3	21,3	75,1	5,1	0,7	35,5	1,9
MA329_L1	21583910	21199963	233184	213255	8,5	1,1	58,0		1,0		
MA329_L1_CAP	70696059	69558758	10464839	1373532	86,9	15,0	63,8	5,8	1,9	13,7	2,0
MA339_L1	15433932	15263727	124190	122941	1,0	0,8	60,0		0,8		
MA339_L1_CAP	34969241	34758511	3512522	1761127	49,9	10,1	63,9	3,9	5,0	12,4	6,3
MA352_L1	15137386	14835833	101196	98460	2,7	0,7	59,9		0,7		
MA352_L1_CAP	38345282	37792220	2268882	935587	58,8	6,0	61,3	1,4	2,4	8,8	3,8
MA384_L1	24545511	24043513	229246	212599	7,3	1,0	67,7		0,9		
MA384_L1_CAP	38339214	37875421	1916971	825039	57,0	5,1	69,7	2,0	2,2	5,3	2,5
MA519_L1	4794948	4408035	44357	43250	2,5	1,0	67,1		0,9		
MA519_L1_CAP	26698707	26159818	8870705	82902	99,1	33,9	76,2	9,1	0,3	33,7	0,3
MA593_L1	9160987	8811979	61451	57281	6,8	0,7	78,0		0,6		
MA593_L1_CAP	27485961	26998834	1400383	139834	90,0	5,2	80,1	2,1	0,5	7,4	0,8
MA629_L1	24533894	23301094	121578	101560	16,5	0,5	56,0		0,4		
MA629_L1_CAP	60319857	58404682	4643960	651873	86,0	8,0	60,5	4,5	1,1	15,2	2,6
MA632_L2	14280141	13607031	116433	110970	4,7	0,9	63,7		0,8		
MA632_L2_CAP	38085503	37443192	5936543	844362	85,8	15,9	67,6	3,9	2,2	18,5	2,9
MA656_L2	52376252	44887890	344839	256328	25,7	0,8	53,2		0,5		
MA656_L2_CAP	58796373	54838412	4193996	574858	86,3	7,6	55,9	2,7	1,0	10,0	2,0
MA686_L1	10626562	9868945	53755	49091	8,7	0,5	58,4		0,5		
MA686_L1_CAP	45575909	43126878	2797793	339323	87,9	6,5	61,8	3,4	0,7	11,9	1,6
MA719_L1	16781155	15445464	86619	73731	14,9	0,6	59,0		0,4		
MA719_L1_CAP	42251001	41545976	2497043	13114	99,5	6,0	64,8	5,8	0,0	10,7	0,1
MA723_L1	10703122	9848602	50209	46116	8,2	0,5	66,5		0,4		
MA723_L1_CAP	42303032	39901972	1779843	312266	82,5	4,5	70,5	4,0	0,7	8,7	1,7
MA728_L1	9773156	8714755	95601	86031	10,0	1,1	62,8		0,9		
MA728_L1_CAP	52413753	47723605	5787098	491460	91,5	12,1	60,2	-2,6	0,9	11,1	1,1
MA886_L1	35910845	11333435	58725	58646	0,1	0,5	39,8		0,2		
MA886_L1_CAP	121793025	58027947	1658777	72887	95,6	2,9	40,4	0,6	0,1	5,5	0,4
MA889_L1	23959874	15794870	94563	91874	2,8	0,6	47,1		0,4		
MA889_L1_CAP	40680948	27372849	375997	211191	43,8	1,4	47,0	-0,1	0,5	2,3	1,4
MA891_L1	62233862	30512252	292202	291122	0,4	1,0	41,4		0,5		
MA891_L1_CAP	71537048	47002040	3702614	389070	89,5	7,9	46,5	5,1	0,5	8,2	1,2
MA900_L1	29402312	23651442	108831	108024	0,7	0,5	48,2		0,4		
MA900_L1_CAP	60711139	52104106	1559522	458901	70,6	3,0	47,9	-0,3	0,8	6,5	2,1
MA907_L2	9568499	7224612	36202	31275	13,6	0,5	47,0		0,3		
MA907_L2_CAP	64629605	54228602	2107082	122690	94,2	3,9	45,6	-1,4	0,2	7,8	0,6
MA910_L1	42914583	36599739	187944	151877	19,2	0,5	52,5		0,4		
MA910_L1_CAP	50096052	45273016	1587970	336350	78,8	3,5	53,5	1,0	0,7	6,8	1,9
Average								3,2		13,0	2,6

References

1 Rasmussen, M. *et al.* Ancient human genome sequence of an extinct Palaeo-Eskimo. *Nature* **463**, 757-762, doi:10.1038/nature08835 (2010).

2 Willerslev, E. & Cooper, A. Ancient DNA. *Proceedings of the Royal Society B-Biological Sciences* **272**, 3-16, doi:10.1098/rspb.2004.2813 (2005).

3 Gilbert, M. T. P., Bandelt, H. J., Hofreiter, M. & Barnes, I. Assessing ancient DNA studies. *Trends in Ecology & Evolution* **20**, 541-544, doi:10.1016/j.tree.2005.07.005 (2005).

4 Damgaard, P. d. B. *et al.* Improving access to endogenous DNA in ancient bones and teeth. *bioRxiv* (2015).

5 Rohland, N. & Hofreiter, M. Comparison and optimization of ancient DNA extraction. *Biotechniques* **42**, 343-352, doi:10.2144/000112383 (2007).

6 Orlando, L. *et al.* Recalibrating Equus evolution using the genome sequence of an early Middle Pleistocene horse. *Nature* **499**, 74-78, doi:10.1038/nature12323 (2013).

7 Dabney, J. *et al.* Complete mitochondrial genome sequence of a Middle Pleistocene cave bear reconstructed from ultrashort DNA fragments. *Proceedings of the National Academy of Sciences* **110**, 15758-15763, doi:10.1073/pnas.1314445110 (2013).

8 Meyer, M. & Kircher, M. Illumina Sequencing Library Preparation for Highly Multiplexed Target Capture and Sequencing. *Cold Spring Harbor Protocols* **2010**, pdb.prot5448, doi:10.1101/pdb.prot5448 (2010).

9 Carpenter, Meredith L. *et al.* Pulling out the 1%: Whole-Genome Capture for the Targeted Enrichment of Ancient DNA Sequencing Libraries. *American Journal of Human Genetics* **93**, 852-864, doi:10.1016/j.ajhg.2013.10.002 (2013).

10 Avila-Arcos, M. *et al. Comparative Performance of Two Whole Genome Capture Methodologies on Ancient DNA Illumina Libraries*. (2014).

Section 4

Radiocarbon dating

The vast majority of radiocarbon dates in this project have been obtained from the Oxford Radiocarbon Accelerator Unit (ORAU) at the University of Oxford.

Oxford Laboratory methods:

The ORAU AMS dating bone using the following chemical pretreatment protocol:

- Coarsely ground bone powder was loaded into a glass test tube;
- A sequence of 0.5 M HCl, 0.1M NaOH and 0.5M HCl was used to treat the bone, interspersed with rinsing with ultra-pure (MilliQ™) water between each reagent;
- Crude collagen was gelatinised in pH3 solution at 75°C for 20 hours;
- The gelatin solution was filtered using a polyethylene Eezi-filter™ whose pore size ranges between 45-90 mm, that is precleaned by thorough rinsing and ultrasonication and the insoluble residues discarded;
- the filtered gelatin was then pipetted into a precleaned ultra-filter (Vivaspin™ 15 30kD MWCO) and centrifuged at 2500-3000 rpm until 0.5-1 mL of the >30 kD gelatin fraction remains (typically 20—40 min)(for the human bone this was not applied due to the low sample size of the recovered collagen);
- This gelatin was freeze-dried ready for combustion in a CHN analyser.

The ultrafiltration step was originally described by Brown *et al.*[1] and the ORAU as used the Sartorius and Vivaspin filters since 2000. The precleaning steps are undertaken after the protocols outlined in[2].

Combusted gelatin samples were analysed using a PDZ-Europa Robo-Prep biological sample converter (combustion elemental analyser) coupled to a PDZ-Europa 20/20 mass spectrometer operating in continuous flow mode using an He carrier gas. This enables $d^{15}N$ and $d^{13}C$, nitrogen and carbon content and calculation of C:N atomic ratios. VPDB is the standard for $d^{13}C$ values. Graphite was produced by reacting the sample CO_2 over an iron catalyst in an excess H_2 atmosphere at 560°C. AMS radiocarbon measurement was carried out using the ORAU 2.5MV HVEE accelerator.

Radiocarbon dates of bone are reported in Supplementary Table 1. All bones/teeth were well preserved in terms of collagen, with only one <than 1% wt. collagen (the effective threshold in the ORAU). All other analytical parameters measured, including the carbon to nitrogen atomic ratio, were acceptable.

We used OxCal 4.2.2[3] and the INTCAL09 calibration curve[4] to calibrate the radiocarbon data.

References

1 Brown, T. A., Nelson, D. E., Vogel, J. S. & Southon, J. R. Improved collagen extraction by modified Longin method. *Radiocarbon* **30**, 171-177 (1988).

2 Brock, F., Higham, T., Ditchfield, P. & Bronk Ramsey, C. Current pretreatment methods for AMS radiocarbon dating at the Oxford Radiocarbon Accelerator Unit (ORAU). *Radiocarbon* **52**, 103-112 (2010).

3 Ramsey, C. B. Development of the radiocarbon calibration program. *Radiocarbon* **43**, 355-364 (2001).

4 Reimer, P. J. *et al.* IntCal13 and Marine13 radiocarbon age calibration curves 0-50,000 years cal BP. (2013).

Section 5

Bioinformatics and DNA authentication

5.1 Bioinformatics

The Illumina data was basecalled using Illumina software CASAVA 1.8.2 and sequences were de multiplexed with a requirement of full match of the 6 nucleotide index that was used for library preparation. Adapter sequences and leading/trailing stretches of Ns were trimmed from the reads and additionally bases with quality 2 or less were removed using AdapterRemoval-1.5.4. Trimmed reads of at least 30 bp were mapped to the human reference genome build 37 using bwa-0.6.2[1] with the seed disabled to allow for higher sensitivity[2]. Mapped reads were filtered for mapping quality 30 and sorted using Picard (http://picard.sourceforge.net) and samtools[3]. Data was merged to library level and duplicates removed using Picard MarkDuplicates (http://picard.sourceforge.net) and hereafter merged to sample level. Sample level BAMs were re-aligned using GATK-2.2-3 and hereafter had the md-tag updated and extended BAQs calculated using samtools calmd[3]. Read depth and coverage were determined using pysam (http://code.google.com/p/pysam/) and BEDtools[4]. Statistics of the read data processing is shown in Supplementary Table 6.

DNA sequence alignments are available from the European Nucleotide Archive (http://www.ebi.ac.uk/ena) under accession number PRJEB9021.

5.2 DNA damage

DNA degrades over time and ancient DNA can therefore be characterised by certain types of damages that are not expected to be present in modern DNA. These serve as important validation criteria an aDNA research[5-7]. First of all the bulk of the template molecules are expected to be relatively short as the DNA strand breaks at a certain rate governed in part by the ambient temperature[8]. Moreover, a high frequency of cytosine deamination resulting in apparent C → T transitions towards the 5' end (when compared to the human reference genome) is a typical characteristic of ancient DNA. Lastly, ancient DNA is expected to display long single stranded overhangs.

Using the Bayesian approach implemented in mapDamage 2.0[7] we recorded the following three key damage parameters for each sample: 1) the frequency of C → T transitions at the first position at the 5' end of reads, 2) λ, the fraction of bases positioned in single-stranded overhangs, and 3) δs, the estimated C → T transition rate in the single-stranded overhangs. MapDamage ouputs were retrieved and analysed with R scripts, and the results are summarized in the Supplementary Table 7.

Among the 102 samples (101 individuals), the observed C → T frequency in the 5' end ranged from 10.1% to 40.4% (average = 20.3%), the estimated fraction of bases found in single stranded overhangs (λ) ranged from 29% to 54% (mean = 42%) and the C → T transition rate in the single-stranded overhangs (δs) ranged from 25% to 100% (mean = 62%)

(Supplementary Table 7). These values indicate that the DNA in all samples is highly degraded and at least the bulk of the template molecules are very likely to be of ancient origin.

These results cannot, however, completely exclude a certain level of modern DNA contamination, why it is also necessary to perform actual contamination estimates in cases where there is sufficient data to do so.

5.3 DNA contamination and sex determination

We estimated the DNA contamination fraction with two different methods that rely on similar principles. The idea is to consider "polymorphic" positions in chromosomes appearing in only one copy in the genome (namely the MT-chromosome for all samples and the X-chromosome for males). In those cases, one expects a single allele at each site on that chromosome (if one disregards heteroplasmy in the MT and the small part where the X-chromosome is homologous with the Y chromosome). Reads that cover the same position but do not contain the same base must therefore either be due to errors (sequencing or mapping) or contamination, i.e., reads that derive from other individuals than the one sampled.

Note that the advantage in using the MT is that the depth of coverage on this chromosome tends to be higher than any other chromosome since cells have generally multiple copies of the organelle. So although this chromosome is fairly short, the number of reads covering each position is much higher, making it feasible to obtain a contamination estimate for data at low depth over the whole genome. Moreover, the MT presumably does not recombine, so one can capitalize on the linkage information. In contrast, the X-chromosome is much longer and contains more sites that can be informative/polymorphic sites in human populations. Moreover, the X-based estimate provides an autosomal based estimate – which is more relevant for most downstream analyses.

mtDNA based estimates: method and results

To estimate the contamination fraction on the MT, we used a method (contamMix 1.0-10) of Fu et al.[9] that generates a moment-based estimate of the error rate and a Bayesian-based estimate of the posterior probability of the contamination fraction.

We mapped the reads from each sample to the nuclear genome (genome build 37.1) as well as to the MT rCRS[10]. For the samples with sufficient coverage (i.e. a MT depth of 10X and above) we retained the reads that mapped to the rCRS with a mapping quality above 30, which in principle should reduce the effect of "nuclear mitochondrial DNA" (numts). We then called a consensus sequence using ANGSD[11] (0.615) for positions covered by 5 reads and above to reduce the effect of damage and filtering out bases with a quality below 20 (-setMinDepth 5 -doFasta 2 -doCounts 1 –minQ 20). We aligned the consensus sequence to a set of 311 human sequences as was done in Fu et al.[9]. We ran contamMix using for input the aligned of 312 sequenced and the reads mapping to the rCRS and running three chains of 50,000 iterations for the Monte Carlo Markov Chain and discarded the first 10,000, as was done in Fu et al[9] and trimming 5bp from each ends of the reads (--trimBases 5). We assessed

convergence of the chains by visualizing the potential scale reduction factor (PSRF) and verifying that the median of PSRF is below 1.1 for all cases[12,13].

We conservatively excluded samples with maximum a posteriori (MAP) contamination probabilities above 5%. This resulted in a total dataset of 102 samples (101 individuals), including 15 samples that were not tested due to less than 10X coverage on the MT. The average estimated contamination proportion for the remaining 87 individuals was 1.8% (Suplementary Table 8).

X chromosomes based estimates: method and results

For the 7 samples determined to be males and for which there is sufficient coverage on the X chromosome, namely a depth of coverage above 0.5X, we estimated the contamination rate with a maximum likelihood based method, which is described in detail in previous work Rasmussen et al[14] and as implemented in the package ANGSD (0.615). We ran the method with default parameters after trimming 5bp form each end of the reads to reduce the effect of ancient DNA damage. We used the CEU HapMap population as a reference population. Since both methods implemented in ANGSD produced essentially identical results for all the 7 samples, we report the results for method 1. In each case the null hypothesis of no contamination was rejected at a 5% level, while all maximum likelihood estimates were between 0.0% and 1.4% with an average value of 0.6% (Supplementary Table 8).

Genetic sex determination

We used the ratio of reads mapping to Y and the X chromosome to determine the sex of each sample as described in Skoglund et al[15]. To do so, we calculated the fraction of reads that map to the Y chromosome out of the total of reads mapping to both the Y and the X chromosome which in turn is used to assign the sample to either XX or XY. Results are shown in Supplementary Table 1.

References

1 Li, H. & Durbin, R. Fast and accurate short read alignment with Burrows–Wheeler transform. *Bioinformatics* **25**, 1754-1760, doi:10.1093/bioinformatics/btp324 (2009).

2 Schubert, M. *et al.* Improving ancient DNA read mapping against modern reference genomes. *BMC Genomics* **13**, 178 (2012).

3 Li, H. *et al.* The Sequence Alignment/Map format and SAMtools. *Bioinformatics* **25**, 2078-2079, doi:10.1093/bioinformatics/btp352 (2009).

4 Quinlan, A. R. & Hall, I. M. BEDTools: a flexible suite of utilities for comparing genomic features. *Bioinformatics* **26**, 841-842, doi:10.1093/bioinformatics/btq033 (2010).

5 Briggs, A. W. *et al.* Patterns of damage in genomic DNA sequences from a Neandertal. *Proceedings of the National Academy of Sciences of the United States of America* **104**, 14616-14621, doi:10.1073/pnas.0704665104 (2007).

6 Sawyer, S., Krause, J., Guschanski, K., Savolainen, V. & Pääbo, S. Temporal Patterns of Nucleotide Misincorporations and DNA Fragmentation in Ancient DNA. *PLoS ONE* **7**, e34131, doi:10.1371/journal.pone.0034131 (2012).

7 Jónsson, H., Ginolhac, A., Schubert, M., Johnson, P. & Orlando, L. mapDamage2.0: fast approximate Bayesian estimates of ancient DNA damage parameters. *Bioinformatics*, doi:10.1093/bioinformatics/btt193 (2013).
8 Allentoft, M. E. *et al.* The half-life of DNA in bone: measuring decay kinetics in 158 dated fossils. *Proceedings of the Royal Society B: Biological Sciences* **279**, 4724-4733, doi:10.1098/rspb.2012.1745 (2012).
9 Fu, Q. M. *et al.* DNA analysis of an early modern human from Tianyuan Cave, China. *Proceedings of the National Academy of Sciences of the United States of America* **110**, 2223-2227, doi:Doi 10.1073/Pnas.1221359110 (2013).
10 Andrews, R. M. *et al.* Reanalysis and revision of the Cambridge reference sequence for human mitochondrial DNA. *Nat Genet* **23**, 147-147 (1999).
11 Korneliussen, T. S., Albrechtsen, A. & Nielsen, R. ANGSD: Analysis of Next Generation Sequencing Data. *Bmc Bioinformatics* **15**, doi:Artn 356
Doi 10.1186/S12859-014-0356-4 (2014).
12 Plummer, M., Best, N., Cowles, K. & Vines, K. CODA: Convergence diagnosis and output analysis for MCMC. *R news* **6**, 7-11 (2006).
13 Gelman, A. & Rubin, D. B. Inference from iterative simulation using multiple sequences. *Statistical science*, 457-472 (1992).
14 Rasmussen, M. *et al.* An Aboriginal Australian Genome Reveals Separate Human Dispersals into Asia. *Science* **334**, 94-98, doi:Doi 10.1126/Science.1211177 (2011).
15 Skoglund, P. *et al.* Origins and Genetic Legacy of Neolithic Farmers and Hunter-Gatherers in Europe. *Science* **336**, 466-469, doi:10.1126/science.1216304 (2012).

Section 6

Population genomics

6.1 Datasets

We constructed two datasets for population genetic analysis by merging ancient DNA data generated in this as well as previous studies with a reference panel of modern individual genotype data. For both datasets, genotypes for all ancient individuals were obtained at all variant positions in the reference panel, discarding variants where alleles for the ancient individuals did not match either of the alleles observed in the panel. All individuals in this study as well as the majority of the previously published ones are low coverage data. For those, we used the 'mpileup' command of samtools[1] (https://github.com/samtools/samtools) to extract reads overlapping the variants, then randomly sampling a single read with both mapping and base quality ≥ 30. For higher coverage individuals we called genotypes using the 'call' command of bcftools[2] (https://github.com/samtools/bcftools) and filtering for quality score (QUAL) ≥ 30.

Affymetrix Human Origins SNP array dataset

This dataset consists of 2,345 contemporary humans from 203 populations genotyped at 594,924 autosomal SNPs, as well as 11 ancient individuals[3]. We additionally merged ancient individuals from the following studies:

(1) A 45,000 year-old Paleolithic individual from Siberia (Ust' – Ishim), sequenced to high coverage[4]
(2) A 36,000 year-old Paleolithic individual from Russia (Kostenki)[5]
(3) Thirteen individuals from Hungary[6] spanning the Neolithic, Bronze Age and Iron Age, of which two individuals (NE1, BR2) were high coverage.
(4) Two individuals from Neolithic Sweden (Ajv58, Gok2)[7]

1000 Genomes whole-genome sequencing dataset

This dataset is based on the initial callset of phase 3 of the 1000 Genomes project[8] (ftp://ftp.1000genomes.ebi.ac.uk/vol1/ftp/release/20130502/). We used a subset of the callset including 10 random unrelated individuals from each of the 26 populations, consisting of an initial callset of 22,887,102 autosomal SNPs. We furthermore applied the following filters to minimize the influence of sequencing artefacts and ascertainment bias:

- We restricted the analysis to regions in the 'accessible genome' as defined by the 1000 Genomes project 'strict' mask (ftp://ftp.1000genomes.ebi.ac.uk/vol1/ftp/release/20130502/supporting/accessible_genome_masks/20141020.strict_mask.whole_genome.bed)

- We used only SNPs that were found to be polymorphic in an outgroup population (Yoruba).
- We used only transversion SNPs

The final dataset after filtering contained a total of 2,542,770 SNPs.

In addition to the ancient individuals described for the Affymetrix Human Origins SNP array dataset, we merged the following individuals:

(1) A 24,000 year-old Paleolithic individual from Siberia (Mal'ta)[9]
(2) Individuals from Western and Northern Europe[3], two of which were sequenced to high coverage (Loschbour, Stuttgart). Data from six low-coverage individuals from Motala, Sweden were merged into a single individual following the original study.
(3) A 7,000 year-old Mesolithic individual from Spain (La Braña)[10]
(4) The Tyrolean Iceman, a 5,300 year-old Copper Age individual from Northern Italy[11]

For population genetic analyses (D- and *f*-statistics, F_{ST}) we obtained sample allele frequencies for the ancient groups (Supplementary Table 9) at each SNP by counting the total number of alleles observed, treating the low coverage individuals as haploid.

6.2 Error analysis for low coverage individuals

Many individuals in our dataset are low coverage data with less than 1X genomic coverage. We therefore performed the following error analysis in order to determine the effect of low coverage on the population genomic inferences and to establish a coverage cut-off for inclusion of individuals. We initially obtained genotypes for all ancient individuals with >0.01X coverage using the Human Origins dataset (panel A), as described above. We then selected the individual with the largest number of SNPs for each ancient group, requiring a minimum of 300,000 SNPs, as well as all high-coverage individuals from previous studies (Ust-Ishim, Loschbour, Stuttgart, NE1, BR2). This yielded a total of 17 test individuals, distributed across 16 groups. For each individual, we then generated 12 datasets with increasingly lower coverage by randomly sampling SNPs. The subsampled individuals were analysed using principal component analysis and ADMIXTURE as described below. Per-individual error rates for the ADMIXTURE analysis were calculated as root mean square error (RMSE) across all observed cluster proportions over all values of K.

We find that errors are comparably low with as few as 20,000 SNPs (all RMSE < 0.05), but start to increase more substantially for datasets with less than 10,000 SNPs (Supplementary Figures 2-4). However, the increasing error below 20,000 SNPs mostly relates to an increased uncertainty in the proportion of the same ancestral clusters observed in the full data, rather than wrongly assigned clusters. Based on this analysis, we therefore required a minimum of 10,000 SNPs for inclusion in the final dataset, and mark individuals with <20,000 SNPs in the ADMXTURE results in order to indicate higher uncertainty in the cluster proportions.

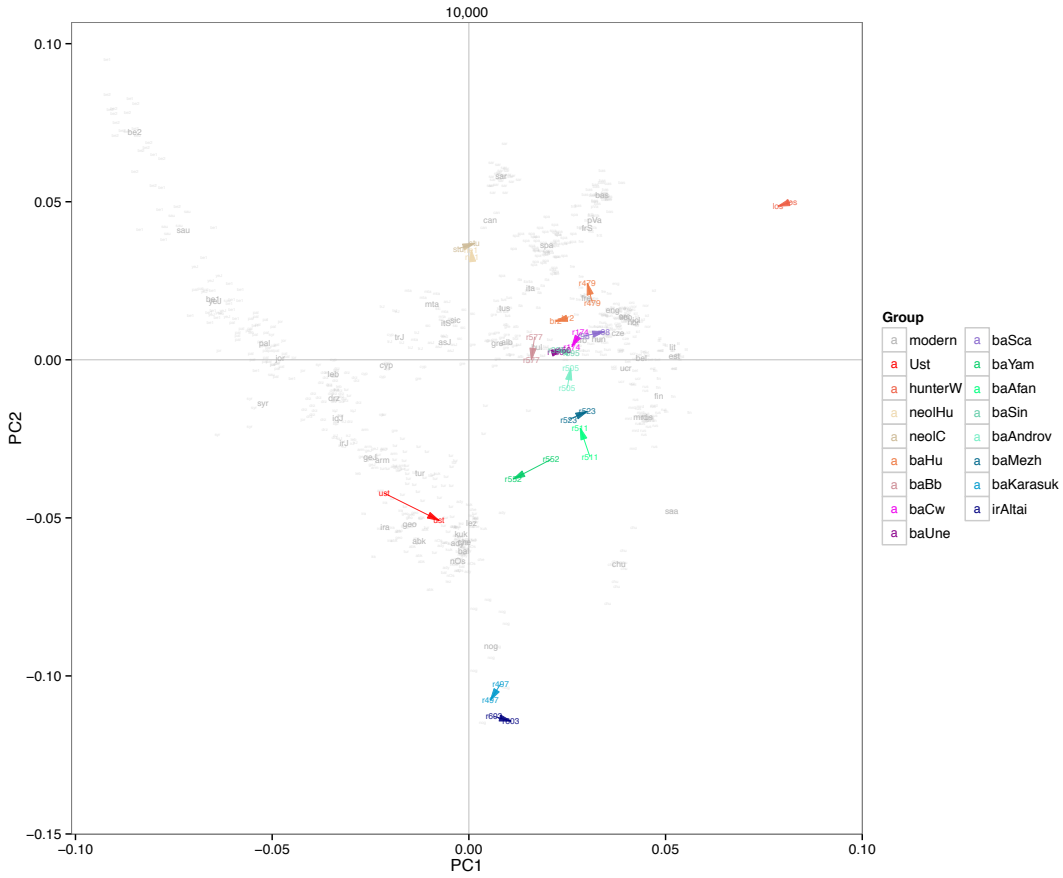

Supplementary Figure 2. Example of principal component analysis of individuals subsampled to 10,000 SNPs. Arrows indicate the shift in position for each ancient individual compared to the full dataset.

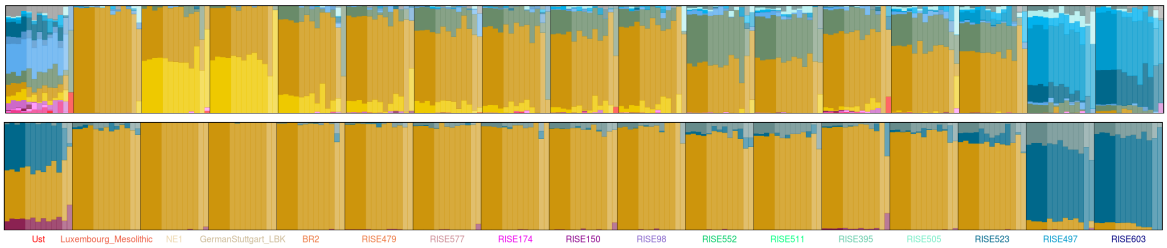

Supplementary Figure 3. Example of ADMIXTURE results for subsampled individuals for K=4 and K =16. For each individual, cluster proportions are shown for the full data and subsampled datasets with decreasing number of SNPs from left to right. Medium shading indicates datasets with 100,000 ≤ N_{SNPs} ≤ 10,000, light shading with N_{SNPs} < 10,000.

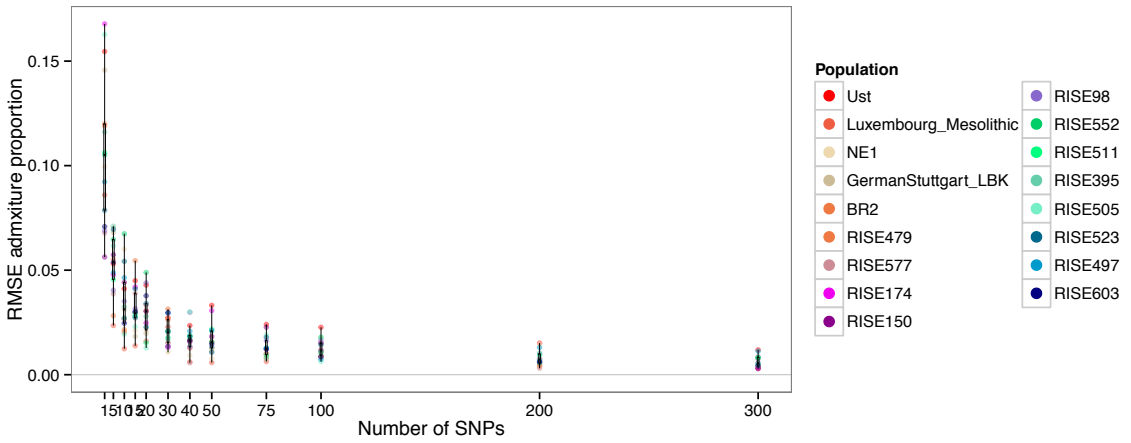

Supplementary Figure 4. RMSE for individual ADMIXTURE proportions for different subsets of SNPs.

6.3 Principal component analysis

We performed principal component analysis on two subsets of individuals from the Human Origins dataset, one including all non-African populations, and another more regional set of all populations from West Asia, Europe and the Caucasus (Extended Data Fig. 1). Principal component analysis was performed with EIGENSOFT[12], projecting ancient individuals onto the components inferred from these sets of modern individuals by using the 'lsqproject' option of *smartpca*. The dataset was converted to all homozygous genotypes prior to the analysis, by randomly sampling an allele at each heterozygote genotype of modern and high-coverage ancient individuals.

To determine which individuals cluster together in the PCA, we performed a clustering analysis using affinity propagation clustering, a recent approach that does not require a-priori specification of the expected number of clusters[13]. We performed clustering on the first 10 PCs inferred from the non-African populations, using the R package *apcluster*. The number of input PCs was chosen by visual inspection of the PCA results, discarding all higher PCs which appeared uninformative about broad-scale between-population patterns. We identified a total of 11 clusters, largely corresponding to geographical and cultural context of the individuals (Supplementary Figure 5). Between-cluster similarity is high for many BAE, whereas earlier contexts often show lower similarity (e.g. Mesolithic hunter-gatherers, Neolithic farmers) indicating higher population stratification among pre-Bronze Age groups.

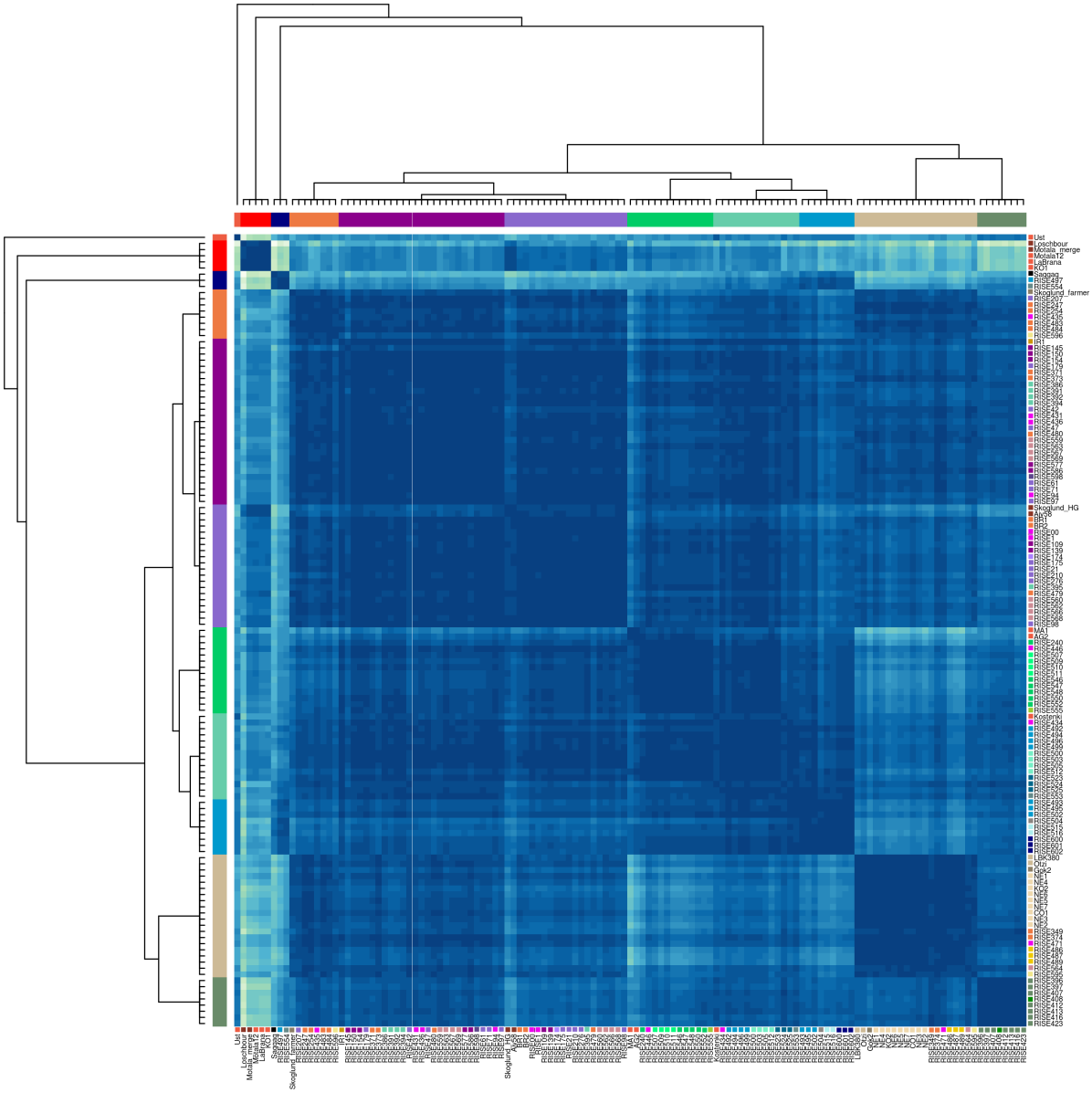

Supplementary Figure 5. Heat map of between-individual similarity from AP clustering.

Pairwise similarity is indicated by blue shading, with dark blue corresponding to higher similarity. Coloured bars indicate cluster membership, with colours corresponding to group colours of majority cluster members. Coloured symbols indicate group for each ancient individual.

6.4 Model-based clustering (ADMIXTURE)

We performed model-based clustering analysis using the maximum-likelihood approach implemented in ADMIXTURE[14]. The majority of the ancient individuals are low coverage, which prohibits running ADMIXTURE jointly on both modern and ancient samples due to the fact that few if any SNPs would be non-missing in all ancient samples. To overcome this

limitation, we used an approach where we first infer the ancestral components using modern samples only, and then "project" the ancient samples onto the inferred components using the ancestral allele frequencies inferred by ADMIXTURE (the 'P' matrix)[15]. This approach has the additional advantage of avoiding possible biases due to correlations between ancient samples due to factors not related to the underlying genetic structure, such as shared ancient DNA damage patterns.

We ran ADMIXTURE on an LD-pruned dataset of all 2,345 modern individuals in the Human Origins SNP array dataset, generated using PLINK with the flag '--indep-pairwise 200 25 0.4', which resulted in a total of 290,310 autosomal SNPs included in the analysis. We assumed K=2 to K=20 ancestral components, and selected the best of 50 replicate runs for each value of K to infer the ancestral composition for the ancient individuals. Genotypes where the ancient individuals show the damage allele at C>T and G>A SNPs were excluded for each low coverage ancient individual.

As we use this analysis as an exploratory tool for identifying the genetic affinities of the ancient individuals, we did not perform cross-validation to identify an "optimal" number of clusters in the dataset, and rather report the full results for all assumed K values. Below we discuss in more detail each K values where we observe a substantial change in the ancestry composition of the BAE individuals (Supplementary Figure 6).

K = 2

Africans separate from non-Africans, BAE are non-African

K = 3

A component separating West Eurasia from East Asians / Native American appears. BAE are mostly West Eurasian, some with low levels of this component. However we also observe some later BA Asians with majority East Asian / Native American ancestry

K = 4

East Asians and Native Americans separate. Many BAE that previously showed low levels of East Asian ancestry (e.g. Yamnaya) now appear Native American, whereas late BA individuals with higher proportions derive from both these components. Individuals from the Okunevo culture show the highest proportion of Native American ancestry.

K = 6

Populations from Oceania form their own component, which is present at low levels in BA Armenians and Yamnaya / Afanasievo, as well as some later BA Asians.

K_= 7

A component maximized in Far East Siberian populations such as Itelmen and Koryak. The East Asian ancestry fraction in most BA Asians is now dominated by this Siberian component.

K = 8

A component maximized in South Asians such as Mala, also present at substantial fraction in Central Asian populations and to a lower extent in the Caucasus. BA Armenians and Yamnaya / Afanasievo now derive ~20% of their ancestry from this component.

K = 9

A component maximized in West Asian populations such as Bedouin appears. Many contemporary Europeans, as well as populations from the Caucasus and Central Asia derive a substantial fraction of their ancestry from this component. This component separates the previously mostly uniform appearing Mesolithic hunter-gatherers from Neolithic farmers, who now appear ~50% West Asian. The distribution of this component is consistent with being a marker for Neolithic Farmer-related ancestry introduced into Europe during the Neolithic transition. Among the BAE we find it at highest frequency in BA Armenians, followed by Hungarians. Low levels are observed in Northern and Central Europeans, as well as Sintashta and possibly Andronova, whereas it is absent in Yamnaya.

K = 12

Native American populations separate into a Northern and Southern component. In BAE with Native American ancestry these components appear roughly evenly split.

K = 14

Siberian ancestry is further separated into a far eastern (Itelmen, Koryak) and northern (Nganasan) component. Siberian ancestry in BAE appears mostly related to Nganasan, with the exception of Okunevo and Afontova Goar and one individual from Karasuk.

K = 15

The previously combined South / Central Asian / Caucasus component splits into a South Asian and a Central Asian / Caucasus component. All BAE with this component show an increase in the Central Asian / Caucasus fraction, and it also appears in BA Hungarians at low frequency.

K =19

The Kalash from Central Asia form their own cluster. Many northern BAE with the Central Asia / Caucasus ancestry now draw part of their ancestry from this component, most notably Yamnaya / Afanasievo, whereas Caucasians increase their fraction of present-day Caucasus-related ancestry.

K = 20

The Bedouin-maximized West Asian component splits into two, the new component maximized in Soutehrn Europe (Sardinia). All ancient samples with previous evidence for the West Asian component relate mostly to the new Southern European component, and

substantially expand their ancestry fractions. Low levels also appear in Mesolithic hunter-gatherers.

In summary, our results suggest the following interpretations:

- Predominantly West Eurasian ancestry for BAE, with the exception of some later BA individuals from Asia, which show influence of ancestry related to present-day Siberians
- A gradual decrease in West-Asia / Neolithic farmer related ancestry from Southern and Central BA Europeans towards the North, which is also present in Armenians but absent from the Northern Caucasus (Yamnaya).
- An opposing gradient in Caucasus / steppe related ancestry, maximized in the Yamnaya and distantly related to Native Americans. Possibly due to the presence of MA1-related ancestry in the Northern Caucasus.
- A genetic link between the Kalash and the steppe through Yamnaya-related people.
- Native American-related ancestry in the Okunevo, possibly due to shared ancestry with paleolihic hunter-gatherers from Mal'ta.

6.5 D- and f-statistics

We used the D- and *f*-statistic framework[16] to investigate patterns of admixture and shared ancestry in our dataset. All statistics were calculated from allele frequencies using the estimators described in Patterson *et al*.[16], with standard errors obtained from a block jackknife with 5Mb block size. We used three types of statistics in the analyses with the following notations

D(Outgroup,Population$_{Test}$)(Population$_1$,Population$_2$)

This D-statistic measures whether the data is consistent with a four-population tree in which Population$_1$ and Population$_2$ form a clade with each other, to the exclusion of the test population and the outgroup. The expected value in case of consistency with the proposed tree is zero. Significant deviations from zero reject the proposed tree, with negative values indicating that the test population is closer to Population$_1$, and positive values indicating that the test population is closer to Population$_2$.

Results from D-statistics are found in Supplementary Table 10.

f_3(Outgroup;Population$_1$,Population$_2$)

This "outgroup"-*f_3* statistic[9] is expected to be proportional to the amount of shared genetic drift between Population$_1$ and Population$_2$ in their common ancestral population until their divergence. Unlike methods based on pairwise distances such as F_{ST}, genetic drift specific to Population$_1$ or Population$_2$ does not affect this statistic.

Results from "outgroup" f_3-statistics are found in Supplementary Table 11.

$f_3(Population_{Test};Population_1,Population_2)$

This is the original formulation of the f_3 statistic as a statistical test for admixture. A significantly negative value of this statistic is evidence for a history of admixture in the test population, related to a pair of source populations $Population_1$ and $Population_2$. A positive value on the other hand does not exclude the possibility of admixture, as drift specific to the test population post-admixture enters adds a positive term to the statistic and can therefore obscure a real historical admixture signal.

Results from "admixture" f_3-statistics are found in Supplementary Table 12.

6.6 Population differentiation (F_{ST})

We investigated population differentiation by estimating F_{ST} for all pairs of ancient and modern groups from allele frequencies using the sample-size corrected moment estimator of Weir and Hill[17], restricting the analysis to SNPs where a minimum two alleles were observed in each population of the pair. While the absolute estimates are likely influenced by small sample sizes and/or other limitations of the ancient data, we expect those effects to be comparable between different ancient groups. We note however that F_{ST} values obtained using both reference datasets are largely consistent and within the expectation given the levels of differentiation observed among present-day populations.

6.7 Phenotypes and positive selection

To investigate the temporal dynamics of SNPs associated with phenotypes or putatively under positive selection, we estimated allele frequencies for a catalogue of 104 SNPs[10] in all ancient and modern groups in the 1000 Genomes dataset (Supplementary Table 13). For this analysis we combined the ancient groups into six broad groups in order to increase sample sizes:

- Palaeolithic
- Hunter-Gatherers
- Neolithic farmers
- BA Europeans
- BA Steppe/Caucasus
- BA Asia

The results from this analysis revealed a surprisingly low frequency of lactase persistence (rs49882350) among BA Europeans. However, the allele frequencies are limited to ancient individuals with sequencing coverage at the SNP of interest. We therefore used imputation to

infer the likely genotype at rs49882350 in all ancient individuals to gain further insight into its distribution among the ancient groups.

Imputation was performed in a 2Mb region centred on rs49882350 following Gamba et al.[6], using the 1000 Genomes Phase 3 data as reference panel. Genotype likelihoods for all ancient samples at the 18,403 SNPs in the region were obtained using the HaplotypeCaller in GATK (version 3.3.0)[18].The likelihoods for C>T and G>A transitions were subsequently set to be equal for all three genotypes in order to minimize possible biases due to DNA damage. Imputation was then performed using Beagle (version 4)[19] with the 1000 Genomes Phase 3 data as reference panel, using 10 iterations for imputation (option 'impute-its=10'). Imputed genotypes with a genotype probability less than 0.85 were excluded for the subsequent analysis.

6.8 Y chromosome analysis and mtDNA haplogroups

Inference of Y chromosome haplogroups for the male individuals was carried out using phylogenetically informative SNPs identified in studies of present-day Y chromosome diversity, as previously described[5,20-22]. We restricted haplogroup assignment to well supported high-level groups corresponding to branches supported by multiple derived alleles.

The mitochondrial consensus sequences were generated using the samtools[1] 'mpileup' function to collect summary information from the mitochondrial bam files and bcftools to output vcf files. In order to by-pass variants derived from DNA damage, the variant list was filtered using a script previously applied in[23], in order to incorporate only bases from positions with > 3 X coverage and > 50 % concordance between the reads into the consensus, excluding indels. The incorporated variants were outputted with a custom Perl script into the HaploGrep[24] hsd format and analysed with the HaploGrep software. The determined haplogroups and quality assignments are listed in Supplementary Table 14.

Supplementary Table 9: Population groupings for ancient individuals

List of the ancient individuals included in the analyses, representing 101 samples from this study and 28 from previous studies (references next to sample name). *Category* refers to the category name used in main text Figures 2 and 3, and *Group name* refer to the abbreviations used in the grouped analyses (Supplementary Tables 10-12). For three samples (RISE174, 408, 504) there were some discrepancy between their archaeological context and their ^{14}C dates, why they have not been assigned to a category, but their admixture proportions are shown in Supplementary Figure 6, and the ^{14}C dating results are listed in Supplementary Table 1. *HG*, hunter-gatherer; *NF*, Neolithic farmer.

Individual	Country	Category	Group name
Ust [4]	Russia	Paleolithic	Ust
Kostenki [5]	Russia	Paleolithic	Kostenki
Afontova_Gora [9]	Russia	Paleolithic	Afontova_Gora
Malta_man [9]	Russia	Paleolithic	Malta_man
Luxembourg_Mesolithic [3]	Luxembourg	Mesolithic HG, West	hunterW
Iberian_Mesolithic [10]	Spain	Mesolithic HG, West	hunterW
KO1 [6]	Hungary	Mesolithic HG, West	hunterW
Swedish_Motala [3]	Sweden	Mesolithic HG, Scandinavia	hunterN
Swedish_Motala_Merge [3]	Sweden	Mesolithic HG, Scandinavia	hunterN
Swedish_hunter_gatherer [7]	Sweden	Mesolithic HG, Scandinavia	hunterN
Ajv58 [7]	Sweden	Mesolithic HG, Scandinavia	hunterN
KO2 [6]	Hungary	NF, Hungary	neolHu
NE1 [6]	Hungary	NF, Hungary	neolHu
NE2 [6]	Hungary	NF, Hungary	neolHu
NE3 [6]	Hungary	NF, Hungary	neolHu
NE4 [6]	Hungary	NF, Hungary	neolHu
NE5 [6]	Hungary	NF, Hungary	neolHu
NE6 [6]	Hungary	NF, Hungary	neolHu
NE7 [6]	Hungary	NF, Hungary	neolHu
CO1 [6]	Hungary	NF, Hungary	neolHu
GermanStuttgart_LBK [3]	Germany	NF, Central	neolC
Tyrolean_Iceman [11]	Italy	NF, Central	neolC
Swedish_farmer [7]	Sweden	NF, Scandinavia	neolN
Gok2 [7]	Sweden	NF, Scandinavia	neolN
RISE486	Italy	Remedello	baRem
RISE487	Italy	Remedello	baRem
RISE489	Italy	Remedello	baRem
BR1 [6]	Hungary	Hungary	baHu
BR2 [6]	Hungary	Hungary	baHu
RISE349	Hungary	Hungary	baHu
RISE479	Hungary	Hungary	baHu
RISE480	Hungary	Hungary	baHu
RISE483	Hungary	Hungary	baHu
RISE484	Hungary	Hungary	baHu
RISE247	Hungary	Hungary	baHu
RISE254	Hungary	Hungary	baHu
RISE371	Hungary	Hungary	baHu
RISE373	Hungary	Hungary	baHu
RISE374	Hungary	Hungary	baHu
RISE559	Germany	Bell Beaker	baBb
RISE560	Germany	Bell Beaker	baBb
RISE562	Germany	Bell Beaker	baBb

RISE563	Germany	Bell Beaker	baBb
RISE564	Germany	Bell Beaker	baBb
RISE568	CzechRep	Bell Beaker	baBb
RISE569	CzechRep	Bell Beaker	baBb
RISE566	CzechRep	Bell Beaker	baBb
RISE567	CzechRep	Bell Beaker	baBb
RISE446	Germany	Corded Ware	baCw
RISE434	Germany	Corded Ware	baCw
RISE435	Germany	Corded Ware	baCw
RISE436	Germany	Corded Ware	baCw
RISE471	Germany	Corded Ware	baCw
RISE431	Poland	Corded Ware	baCw
RISE1	Poland	Corded Ware	baCw
RISE94	Sweden	Corded Ware	baCw
RISE00	Estonia	Corded Ware	baCw
RISE109	Poland	Unetice	baUne
RISE139	Poland	Unetice	baUne
RISE145	Poland	Unetice	baUne
RISE150	Poland	Unetice	baUne
RISE154	Poland	Unetice	baUne
RISE577	CzechRep	Unetice	baUne
RISE586	CzechRep	Unetice	baUne
RISE71	Denmark	Scandinavia	baSca
RISE21	Denmark	Scandinavia	baSca
RISE61	Denmark	Scandinavia	baSca
RISE42	Denmark	Scandinavia	baSca
RISE47	Denmark	Scandinavia	baSca
RISE276	Denmark	Scandinavia	baSca
RISE175	Sweden	Scandinavia	baSca
RISE179	Sweden	Scandinavia	baSca
RISE207	Sweden	Scandinavia	baSca
RISE210	Sweden	Scandinavia	baSca
RISE97	Sweden	Scandinavia	baSca
RISE98	Sweden	Scandinavia	baSca
RISE598	Lithuania	Baltic	baBal
RISE595	Montenegro	Montenegro	baMon
RISE596	Montenegro	Montenegro	baMon
RISE396	Armenia	Armenia	baArm
RISE397	Armenia	Armenia	baArm
RISE407	Armenia	Armenia	baArm
RISE412	Armenia	Armenia	baArm
RISE413	Armenia	Armenia	baArm
RISE416	Armenia	Armenia	baArm
RISE423	Armenia	Armenia	baArm
RISE550	Russia	Yamnaya	baYam

RISE240	Russia	Yamnaya	baYam
RISE546	Russia	Yamnaya	baYam
RISE547	Russia	Yamnaya	baYam
RISE548	Russia	Yamnaya	baYam
RISE552	Russia	Yamnaya	baYam
RISE509	Russia	Afanasievo	baAfan
RISE510	Russia	Afanasievo	baAfan
RISE511	Russia	Afanasievo	baAfan
RISE507	Russia	Afanasievo	baAfan
RISE555	Russia	Stalingrad Quarry	baStq
RISE515	Russia	Okunevo	baOku
RISE516	Russia	Okunevo	baOku
RISE395	Russia	Sintashta	baSin
RISE386	Russia	Sintashta	baSin
RISE394	Russia	Sintashta	baSin
RISE392	Russia	Sintashta	baSin
RISE391	Russia	Sintashta	baSin
RISE500	Russia	Andronovo	baAndrov
RISE503	Russia	Andronovo	baAndrov
RISE512	Russia	Andronovo	baAndrov
RISE505	Russia	Andronovo	baAndrov
RISE523	Russia	Mezhovskaya	baMezh
RISE524	Russia	Mezhovskaya	baMezh
RISE525	Russia	Mezhovskaya	baMezh
RISE495	Russia	Karasuk	baKarasuk
RISE496	Russia	Karasuk	baKarasuk
RISE497	Russia	Karasuk	baKarasuk
RISE499	Russia	Karasuk	baKarasuk
RISE502	Russia	Karasuk	baKarasuk
RISE492	Russia	Karasuk	baKarasuk
RISE493	Russia	Karasuk	baKarasuk
RISE494	Russia	Karasuk	baKarasuk
RISE553	Russia	Afontova Gora	baAfGo
RISE554	Russia	Afontova Gora	baAfGo
RISE602	Russia	Altai	irAltai
RISE600	Russia	Altai	irAltai
RISE601	Russia	Altai	irAltai
IR1 [6]	Hungary	NA	irHu
RISE174	Sweden	NA	irSca
RISE408	Armenia	NA	irArm
RISE504	Russia	NA	irRus
Saqqaq [25]	Greenland	NA	eskimo

References

1 Li, H. *et al.* The Sequence Alignment/Map format and SAMtools. *Bioinformatics* **25**, 2078-2079, doi:10.1093/bioinformatics/btp352 (2009).

2 Li, H. A statistical framework for SNP calling, mutation discovery, association mapping and population genetical parameter estimation from sequencing data. *Bioinformatics* **27**, 2987-2993 (2011).

3 Lazaridis, I. *et al.* Ancient human genomes suggest three ancestral populations for present-day Europeans. *Nature* **513**, 409-413, doi:10.1038/nature13673 (2014).

4 Fu, Q. *et al.* Genome sequence of a 45,000-year-old modern human from western Siberia. *Nature* **514**, 445-449, doi:10.1038/nature13810 (2014).

5 Seguin-Orlando, A. *et al.* Genomic structure in Europeans dating back at least 36,200 years. *Science* **346**, 1113-1118, doi:10.1126/science.aaa0114 (2014).

6 Gamba, C. *et al.* Genome flux and stasis in a five millennium transect of European prehistory. *Nat Commun* **5**, doi:10.1038/ncomms6257 (2014).

7 Skoglund, P. *et al.* Genomic Diversity and Admixture Differs for Stone-Age Scandinavian Foragers and Farmers. *Science* **344**, 747-750, doi:10.1126/science.1253448 (2014).

8 Consortium, G. P. An integrated map of genetic variation from 1,092 human genomes. *Nature* **491**, 56-65 (2012).

9 Raghavan, M. *et al.* Upper Palaeolithic Siberian genome reveals dual ancestry of Native Americans. *Nature* **505**, 87-91, doi:10.1038/nature12736 (2014).

10 Olalde, I. *et al.* Derived immune and ancestral pigmentation alleles in a 7,000-year-old Mesolithic European. *Nature* **507**, 225-228, doi:10.1038/nature12960 (2014).

11 Keller, A. *et al.* New insights into the Tyrolean Iceman's origin and phenotype as inferred by whole-genome sequencing. *Nat Commun* **3**, doi:Artn 698 Doi 10.1038/Ncomms1701 (2012).

12 Patterson, N., Price, A. L. & Reich, D. Population Structure and Eigenanalysis. *PLoS Genet* **2**, e190, doi:10.1371/journal.pgen.0020190 (2006).

13 Frey, B. J. & Dueck, D. Clustering by passing messages between data points. *science* **315**, 972-976 (2007).

14 Alexander, D. H., Novembre, J. & Lange, K. Fast model-based estimation of ancestry in unrelated individuals. *Genome Research* **19**, 1655-1664, doi:10.1101/gr.094052.109 (2009).

15 Sikora, M. *et al.* Population genomic analysis of ancient and modern genomes yields new insights into the genetic ancestry of the Tyrolean Iceman and the genetic structure of Europe. *PLoS genetics* **10**, e1004353 (2014).

16 Patterson, N. J. *et al.* Ancient Admixture in Human History. *Genetics*, doi:10.1534/genetics.112.145037 (2012).

17 Weir, B. S. & Hill, W. Estimating F-statistics. *Annual review of genetics* **36**, 721-750 (2002).

18 McKenna, A. *et al.* The Genome Analysis Toolkit: a MapReduce framework for analyzing next-generation DNA sequencing data. *Genome research* **20**, 1297-1303 (2010).

19 Browning, S. R. & Browning, B. L. Rapid and accurate haplotype phasing and missing-data inference for whole-genome association studies by use of localized haplotype clustering. *The American Journal of Human Genetics* **81**, 1084-1097 (2007).

20 Poznik, G. D. *et al.* Sequencing Y chromosomes resolves discrepancy in time to common ancestor of males versus females. *Science* **341**, 562-565 (2013).

21 Francalacci, P. *et al.* Low-pass DNA sequencing of 1200 Sardinians reconstructs European Y-chromosome phylogeny. *Science* **341**, 565-569 (2013).
22 Underhill, P. A. *et al.* The phylogenetic and geographic structure of Y-chromosome haplogroup R1a. *European Journal of Human Genetics* **23**, 124-131 (2015).
23 Jacobsen, M. W. *et al.* Speciation and demographic history of Atlantic eels (Anguilla anguilla and A. rostrata) revealed by mitogenome sequencing. *Heredity* **113**, 432-442, doi:10.1038/hdy.2014.44 (2014).
24 Kloss-Brandstätter, A. *et al.* HaploGrep: a fast and reliable algorithm for automatic classification of mitochondrial DNA haplogroups. *Human Mutation* **32**, 25-32, doi:10.1002/humu.21382 (2011).
25 Rasmussen, M. *et al.* Ancient human genome sequence of an extinct Palaeo-Eskimo. *Nature* **463**, 757-762, doi:10.1038/nature08835 (2010).

Supplementary Figure 6: Model-based clustering

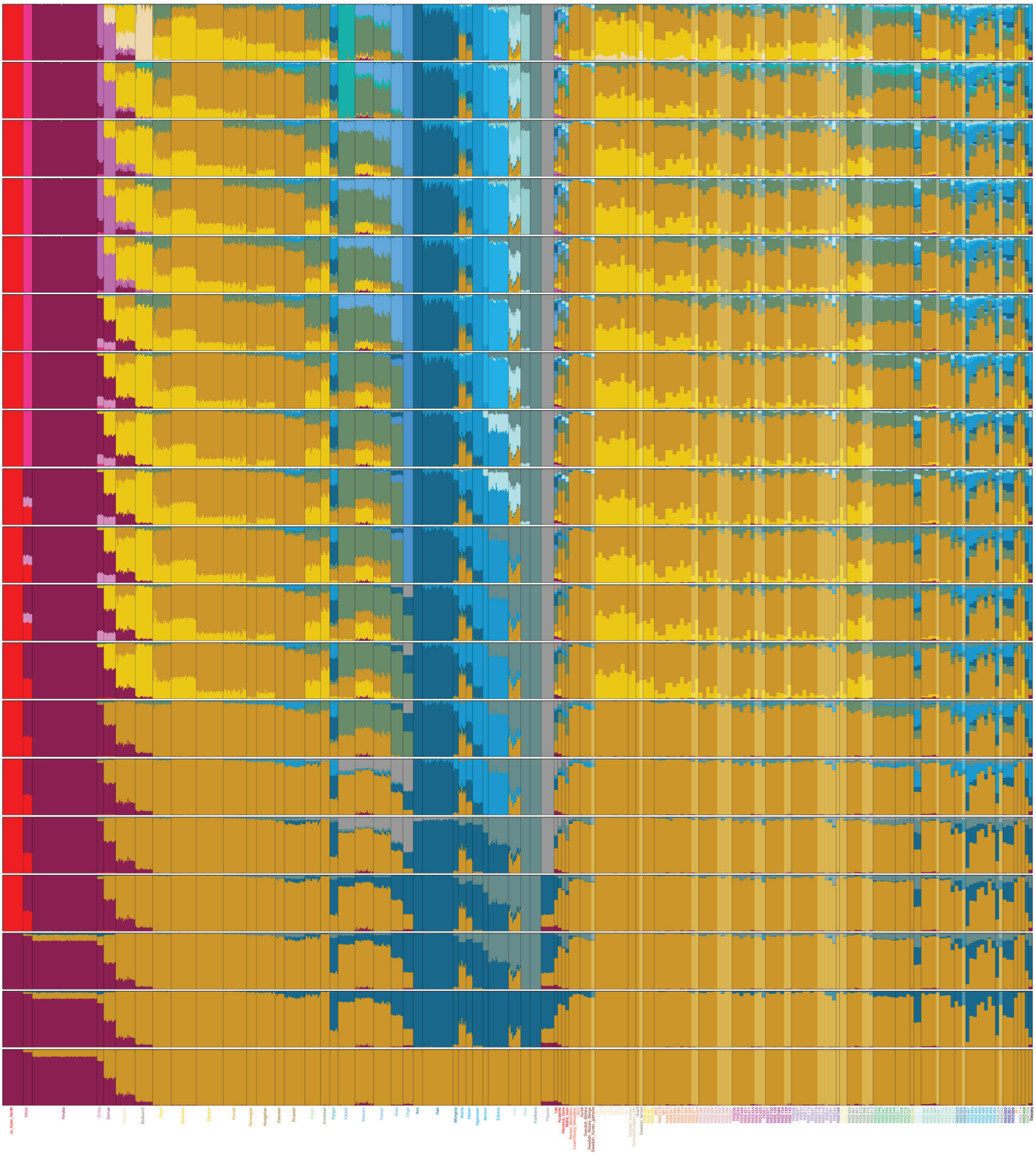

Results from ADMIXTURE for K=2 to K=20 for a representative subset of modern populations and all ancient individuals. Lighter shaded colours indicate individuals with less than 20,000 SNPs overlap.